SJSU SAN JOSÉ STATE UNIVERSITY

MTI MINETA TRANSPORTATION INSTITUTE

Development of Physics-Based Deterioration Models for Reinforced Soil Retaining Structures

Amr M. Morsy, PhD, PE
Islam A. Ebo

CSUTC California State University Transportation Consortium

CALIFORNIA STATE UNIVERSITY LONG BEACH

CSU TRANSPORTATION CONSORTIUM

transweb.sjsu.edu/csutc

MINETA TRANSPORTATION INSTITUTE

Founded in 1991, the Mineta Transportation Institute (MTI), an organized research and training unit in partnership with the Lucas College and Graduate School of Business at San José State University (SJSU), increases mobility for all by improving the safety, efficiency, accessibility, and convenience of our nation's transportation system. Through research, education, workforce development, and technology transfer, we help create a connected world. MTI leads the Mineta Consortium for Equitable, Efficient, and Sustainable Transportation (MCEEST) funded by the U.S. Department of Transportation, the California State University Transportation Consortium (CSUTC) funded by the State of California through Senate Bill 1 and the Climate Change and Extreme Events Training and Research (CCEETR) Program funded by the Federal Railroad Administration. MTI focuses on three primary responsibilities:

Research

MTI conducts multi-disciplinary research focused on surface transportation that contributes to effective decision making. Research areas include: active transportation; planning and policy; security and counterterrorism; sustainable transportation and land use; transit and passenger rail; transportation engineering; transportation finance; transportation technology; and workforce and labor. MTI research publications undergo expert peer review to ensure the quality of the research.

Education and Workforce Development

To ensure the efficient movement of people and products, we must prepare a new cohort of transportation professionals who are ready to lead a more diverse, inclusive, and equitable transportation industry. To help achieve this, MTI sponsors a suite of workforce development and education opportunities. The Institute supports educational programs offered by the Lucas Graduate School of Business: a Master of Science in Transportation Management, plus graduate certificates that include High-Speed and Intercity Rail Management and Transportation Security Management. These flexible programs offer live online classes so that working transportation professionals can pursue an advanced degree regardless of their location.

Information and Technology Transfer

MTI utilizes a diverse array of dissemination methods and media to ensure research results reach those responsible for managing change. These methods include publication, seminars, workshops, websites, social media, webinars, and other technology transfer mechanisms. Additionally, MTI promotes the availability of completed research to professional organizations and works to integrate the research findings into the graduate education program. MTI's extensive collection of transportation-related publications is integrated into San José State University's world-class Martin Luther King, Jr. Library.

Report 24-43

Development of Physics-Based Deterioration Models for Reinforced Soil Retaining Structures

Amr M. Morsy, PhD, PE

Islam A. Ebo

January 2025

A publication of the
Mineta Transportation Institute
Created by Congress in 1991

College of Business
San José State University
San José, CA 95192-0219

TECHNICAL REPORT DOCUMENTATION PAGE

1. Report No. 24-43	**2. Government Accession No.**	**3. Recipient's Catalog No.**	
4. Title and Subtitle Development of Physics-Based Deterioration Models for Reinforced Soil Retaining Structures		**5. Report Date** January 2025 **6. Performing Organization Code**	
7. Authors Amr M. Morsy, PhD, PE ORCID: 0000-0002-9335-7847 Islam A. Ebo ORCID: 0009-0007-6797-8002		**8. Performing Organization Report** CA-MTI-2360	
9. Performing Organization Name and Address Mineta Transportation Institute College of Business San José State University San José, CA 95192-0219		**10. Work Unit No.** **11. Contract or Grant No.** ZSB12017-SJAUX	
12. Sponsoring Agency Name and Address State of California SB1 2017/2018 Trustees of the California State University Sponsored Programs Administration 401 Golden Shore, 5th Floor Long Beach, CA 90802		**13. Type of Report and Period Covered** **14. Sponsoring Agency Code**	
15. Supplemental Notes 10.31979/mti.2024.2360			

16. Abstract

Reinforced soil walls are key earth retention features in the transportation infrastructure. They are used to support and retain soil in a wide variety of crucial structures, such as highways, bridges, and railways, to ensure stability. They also provide solutions for constructing embankments and slopes in constrained spaces, allowing for efficient land use and improved infrastructure planning. This study used advanced numerical modeling to improve the understanding of the behavior and long-term performance of the aging reinforced soil walls from the 1970s for asset management purposes. An asset-scale model was created to simulate the effects of weather on these walls. The model included a system to track how moisture-driven corrosion affects wall stability and performance over time. The model outputs provide implications on the wall progressive deterioration over time and estimates for the wall remaining service life. Unlike newer wall generations constructed with strict specifications that limit fill corrosivity, early wall generations may maintain high levels of moisture for prolonged periods that can significantly increase corrosion rates. Accordingly, it is recommended that fill moisture monitoring be added to asset management measures for early generation walls that could have been constructed with highly corrosive or poorly drainable fills. The results of this study indicate that even though corrosion rates vary with changes in fill moisture, the overall loss in reinforcement thickness happens at a steady rate, showing a linear relationship between cumulative corrosion and time. The results also indicate that 25% fluctuation in fill moisture has no to little effect on the cumulative corrosion, and that the average fill moisture can be used to predict an approximate long-term cumulative corrosion. Thus, it is recommended to use one year of seasonal climate data for a specific location to estimate the annual variation in fill moisture. This can predict the yearly corrosion of reinforcements, which can then be multiplied by the number of service years to estimate long-term cumulative corrosion. Finally, an asset-scale performance model based on performance-requirement failure framework was developed using the outputs of the asset-scale numerical model. These performance models can inform decisions about critical transportation infrastructure maintenance, repair, or replacement strategies, and optimizing resource allocation.

17. Key Words Asset management, Mechanically stabilized earth, Deterioration, Corrosion, Retaining walls.	**18. Distribution Statement** No restrictions. This document is available to the public through The National Technical Information Service, Springfield, VA 22161.		
19. Security Classif. (of this report) Unclassified	**20. Security Classif. (of this page)** Unclassified	**21. No. of Pages** 67	**22. Price**

Form DOT F 1700.7 (8-72)

DOI: 10.31979/mti.2024.2360

Mineta Transportation Institute
College of Business
San José State University
San José, CA 95192-0219

Tel: (408) 924-7560
Fax: (408) 924-7565
Email: mineta-institute@sjsu.edu

transweb.sjsu.edu/research/2360

ACKNOWLEDGMENTS

The work presented in this report was conducted as part of Project 2360, funded by California State University Transportation Consortium (CSUTC) through California Road Repair and Accountability Act of 2017 (SB 1) funds. Amr Morsy recognizes the support of Matthew Barendse of the New York State Department of Transportation (NYSDOT) and Aamir Turk of the Indiana Department of Transportation (INDOT). The authors appreciate the data provided by NYSDOT. The opinions presented in this report are those of the authors and are not necessarily those of the supporting entities. Report cover photo belongs to ©AdobeStock/Michael.

CONTENTS

LIST OF FIGURES

LIST OF TABLES

Executive Summary

Since its advent in the 1960s, soil reinforcement has become an indispensable technology in civil engineering projects providing solutions to earth retention in the US and globally. Reinforced soil retaining walls (also known as Mechanically Stabilized Earth walls or MSE walls) have quickly gained a reputation for being cost-saving, time-efficient, environmental-friendly, and resilient to seismic events, outperforming their conventional counterparts. In current practice, reinforced soil walls represent the substantial majority of all retaining walls constructed in transportation projects. However, none of the reinforced soil walls constructed thus far have yet proven to stand the test of time since the first reinforced soil wall in the US was constructed in California in 1972, which makes it 23 years younger than the 75-year service-life expectancy. Further, design guidelines and construction protocols have evolved significantly since the technology was first adopted in the US in the 1970s. Early-generation reinforced soil walls were constructed using design guidelines and construction protocols that are deemed inadequate according to current practice. Some of these early structures have recently failed unexpectedly because of their deterioration over time.

Reinforced soil retaining walls, like all infrastructure assets, have lifespans beyond which they cease to perform their intended functions. Unexpected, sudden failure of reinforced soil walls can result in severe and costly consequences including traffic disruption, which can impose significant burdens on the limited resources of infrastructure stakeholders. Accordingly, prediction of the remaining service life of existing, aging reinforced soil walls may be necessary to mitigate the consequences associated with unexpected failures.

The service life of a reinforced soil wall is governed by several deterioration mechanisms that may have different onsets and can collectively result in functional failures over time. Deterioration can generally be difficult to quantitatively predict, and it is undoubtedly impossible to predict by visual inspection. Therefore, the service life of reinforced soil walls is often unknown or may be uncertain, which results in excessively expensive risk mitigation measures and inefficient allocation of limited resources. Additionally, the evolution of the specifications for reinforced soil walls—pertaining to the characteristics of reinforced backfill, reinforcement, and galvanization—adds to the uncertainty about the long-term performance and remaining service life of a considerable number of existing early-generation reinforced soil walls.

This study used advanced numerical modeling approaches to offer valuable insights into the behavior and long-term performance of reinforced soil walls for asset management purposes. An asset-scale hydromechanical numerical model was developed for an exemplary reinforced soil wall constructed with metallic reinforcements and a reinforced fill representative of those of early-generation reinforced soil walls. The numerical model considers the soil hydromechanical behavior, which allows prediction of fill moisture fluctuations with time. A material-scale reinforcement model that accounts for moisture-driven corrosion was incorporated in the asset-scale numerical model. This allowed reinforcements to corrode with time at a varying rate in

response to the varying moisture levels within the reinforced fill at the respective location of each reinforcement. Such a numerical model can predict the long-term performance indicators, such as time-dependent soil settlement, reinforcement strains, lateral displacements, and other stability metrics, which are necessary for vulnerability assessment of reinforced soil walls.

The asset-scale numerical model was used to investigate corrosion trends with time for wall cases with wet fills (degree of saturation varying between 75% and 100%) and dry fills (degree of saturation varying between 25% and 50%) based on the water retentivity and hydraulic conductivity of the reinforced fill. The preliminary results of this study indicate that despite the fluctuation of reinforcement corrosion rates associated with the fluctuations of fill moisture, the rate of increase in cumulative thickness loss (i.e., corrosion) with time is fairly constant—that is, the relationship between the cumulative corrosion and time is approximately linear, which is consistent with the corrosion models adopted in current practice. It is notable that the material-scale reinforcement model used in this study conservatively does not consider the formation of rust scales on corroded reinforcements, which tend to slow down the corrosion process with time. In conclusion, the observation of relationship linearity supports current practices that use linear models with time to predict cumulative corrosion.

The results of this study indicate that fill moisture may have a considerable effect on the reinforcement corrosion rate. Unlike newer wall generations constructed with strict specifications that limit fill corrosivity and fines content, early-generation reinforced soil walls may maintain high levels of moisture for prolonged periods that can significantly increase corrosion rates. Accordingly, it is recommended that fill moisture monitoring be added to asset management strategies of early-generation walls that may have been constructed with highly corrosive fills or fills with elevated fines contents. Such data can be useful for making proper predictions based on field conditions. The results of this study also indicate that 25% fluctuation in fill moisture has little to no effect on the cumulative corrosion, and that the average fill moisture (with no fluctuation) can be used to predict long-term cumulative corrosion. Accordingly, it is recommended that average seasonal climate records (one-year average climate records) be used at a given geographic location to produce the one-year variation in fill moisture necessary to predict the amount of corrosion that reinforcements may experience in one year. This predicted value can be multiplied by the number of asset service years to predict the long-term cumulative corrosion.

Finally, an asset-scale performance model based on a performance-requirement failure framework was developed as part of this study using the data obtained from the asset-scale numerical model. In this study, and by way of example, reinforcement tensile strength was used as a performance indicator. As reinforcements progressively corrode and their cross-sections reduce, their tensile strength diminishes to a point where they can no longer sustain the tensile stresses exerted on them by the reinforced fill. Other performance indicators suggested by this study include the rate of lateral displacement, which may be a practical indicator for existing, aged walls that are typically evaluated through monitoring their external deformation over time. These performance models

can serve as decision support tools by providing quantitative data that can inform asset management decision making.

1. Introduction

Since their inception in the 1960s, reinforced soil walls (also known as Mechanically Stabilized Earth walls or MSE walls) have gained a growing reputation for being cost-saving, time-efficient, environmental-friendly, and resilient to seismic events, outperforming their traditional counterparts. Reinforced soil walls have been constructed across the US, majorly by transportation agencies in Arizona, California, Florida, Georgia, New York, North Carolina, Pennsylvania, Texas, and Washington, which are among the largest road-building states (Taylor et al. 2023). As of 2010, the US Federal Highway Administration (FHWA) reported that reinforced soil walls represent more than 50% of all retaining walls constructed in transportation projects (Berg et al. 2009a). However, none of the reinforced soil walls constructed thus far have yet proven to stand the test of time. The first reinforced soil wall in the US was constructed in California in 1972, making it 23 years younger than the 75-year service-life expectancy at the time this report was prepared. Further, design guidelines, construction materials, and protocols have evolved significantly since the technology was first adopted in the US in the 1970s. Early-generation reinforced soil walls were constructed using design guidelines and construction protocols that are deemed inadequate according to the current state of practice. Some of these early walls have recently suffered unexpected failures due to age-related deterioration. Infrastructure stakeholders face challenges in developing and implementing frameworks for assessing the risk associated with the failure of reinforced soil walls and estimating their remaining service life, and thus convenient and efficient methods are needed to identify reinforced soil walls that require attention and dedication of resources for preservation or replacement (Govindasamy et al. 2018).

1.1 Overview of the problem

The performance of reinforced soil wall assets[1] degrades progressively with time through deterioration processes that occur to their constituting components, including fills, reinforcements, facings, and drainage systems. Each component degrades through a number of deterioration mechanisms that contribute variably to the overall deterioration of the asset. For instance, as granular fills age, they creep due to interparticle sliding and delayed particle crushability (Bowman and Soga 2003; Kwok and Bolton 2013; Liu et al. 2019; Gavin and Igoe 2021; Liu et al. 2022). Additionally, fills in reinforced soil walls may be prone to internal erosion by suffusion and induced settlement (Sibille et al. 2015; Breckwoldt et al. 2019), which in turn lead to localized stress concentrations in the reinforcements and overall deterioration in the asset performance.

The reinforcements used in reinforced soil structures are typically metallic or polymeric, both of which are prone to progressive deterioration over time (Elias et al. 2009). Metallic reinforcements

[1] An asset is defined as an infrastructure feature that requires asset management, which is defined by AASTHO (1999) as "a systematic process of maintaining, upgrading, and operating physical assets cost-effectively. It combines engineering principles with sound business practices and economic theory, and it provides tools to facilitate a more organized, logical approach to decision-making."

deteriorate primarily through corrosion at continuously varying rates. Corrosion rates are governed by the electrical conductivity of the fill in which the reinforcements are placed (Nicks et al. 2017; Bronson et al. 2020; Kolay et al. 2020), which depends primarily on fill moisture, concentration of soluble salts (chlorides and sulfates), and pH value (Elias et al. 2009). On the other hand, polymeric reinforcements (i.e., geosynthetics) are prone to installation damage during construction, chemical and biological degradation, and creep (Elias et al. 2009). Installation damage can be correlated to the soil particle characteristics and compaction techniques (Bathurst et al. 2011; Lim and McCartney 2013; Miyata and Bathurst 2015). Chemical and biological degradation may vary from one reinforcement type to another depending on the base polymer used in their manufacturing (e.g., polypropylene, polyethylene, polyester). This degradation is governed primarily by the geosynthetic antioxidant depletion and its rate (e.g., Hsuan and Koerner 1998; Rowe and Sangam 2002; Rowe 2020). Metallic reinforcements were used in the early generations of reinforced soil walls and their deterioration has been the main concern across transportation agencies in recent years (Govindasamy et al. 2018); therefore, this study focused on the deterioration of reinforced soil walls constructed with metallic reinforcements.

Deterioration involves different types of mechanisms that may have different onsets and progress at different rates. Collectively, these mechanisms contribute variably to the overall deterioration rate of an infrastructure asset at a given time during its service life. Consequently, infrastructure stakeholders face challenges in assessing the degree of deterioration in their overwhelmingly large inventories of reinforced soil walls. Additionally, current practice is primarily qualitative and based on visual inspections during intermittent physical field visits, which are incapable of efficiently identifying the retaining walls that are at high risk of imminent failure. Enhanced capabilities are needed to forecast the future performance and the remaining service life of aging walls. This requires robust and reliable modeling approaches that can evaluate the current state of existing walls constructed up to 60 years ago and their remaining service life (Bourgeois et al. 2013). According to the California Transportation Asset Management Plan (TAMP 2022), opportunities identified for future improvements in transportation asset management include "enhancing asset modeling capabilities." Accordingly, this study developed a physics-based asset-scale modeling approach that incorporates material-scale deterioration mechanisms to enable the prediction of the remaining service life of reinforced soil wall assets. This will ultimately enable improved asset management and optimized allocation of resources.

1.2 Research objectives

This study aimed to develop a physics-based deterioration modeling approach for reinforced soil retaining walls with metallic reinforcements to predict their lifecycle performance and remaining service life. The predictions of this model shall enable infrastructure stakeholders to make informed decisions in managing their wall assets. The specific objectives of the study included the following: (1) summarizing the evolution of specifications in reinforced soil walls constructed with metallic reinforcements to identify the attributes of early-generation reinforced soil walls; (2) synthesizing the key deterioration mechanisms in reinforced soil walls constructed with metallic

reinforcements; (3) reviewing and summarizing asset management practices for reinforced soil walls constructed with metallic reinforcements; (4) developing a material-scale deterioration model for wall reinforcements based on experimental and field data available in the literature; (5) developing an asset-scale computational model for reinforced soil walls considering material-scale deterioration; and (6) developing a framework for an asset-scale performance model based on computer model outputs.

1.3 Report organization

This report consists of seven sections:

- Section 1. Introduction: This section presents an overview of the problem and research questions, research aim and objectives, and report organization.
- Section 2. Evolution of Specifications: This section synthesizes the evolution of engineering specifications in reinforced soil walls constructed with metallic reinforcements.
- Section 3. Deterioration of Reinforced Soil Walls: This section synthesizes the key deterioration mechanisms in reinforced soil walls constructed with metallic reinforcements.
- Section 4. Asset Management Practices: This section synthesizes the asset management practices of reinforced soil walls constructed with metallic reinforcements.
- Section 5. Reinforced Soil Wall Computer Model: This section presents a framework for material-scale modeling of reinforcement deterioration and its incorporation into a hydromechanical asset-scale reinforced soil model.
- Section 6. Performance Modeling for Asset Management: This section presents a framework for an asset-scale performance model for aging reinforced soil walls and explains how this model can be used to inform asset management.
- Section 7. Summary and Recommendations: This section summarizes the study documented in this report and provides practical recommendations.

This report was written for infrastructure stakeholders and practicing engineers, with Sections 5 and 6 specifically aimed at practicing engineers.

2. Evolution of Specifications

Modern reinforced soil structures in the form of MSE walls originated in France in the mid-1960s, with the first MSE wall in the US constructed in California in 1972. The recognition and adoption of MSE wall systems progressed gradually through the late 1970s. The earliest Federal Highway Administration (FHWA) design guidance was based on Demonstration Project No. 18 in the mid-1970s (Walkinshaw 1975). The notable expansion of MSE walls in the highway network occurred in the early 1980s, beginning with walls using metallic reinforcements. The American Association of State Highway and Transportation Officials (AASHTO) released its earliest design guidance on MSE walls in the 1990s. As MSE wall systems gained acceptance, the design requirements and construction guidelines for these systems continued to develop. At that time, design and construction specifications had not yet reached the level of maturity seen in current practice. Frondistou-Yannas (1985) was the first study on the corrosion of metallic reinforcements in MSE walls, published 14 years after the first MSE wall in the US was constructed. While the study raised awareness about the importance of corrosion, it was not definitive about the soil property recommendations and precautions against corrosion (Govindasamy et al. 2018).

FHWA Geotechnical Engineering Notebook Guideline No. 1 (FHWA 1987) is considered the first basic reference to provide guidance on the design of MSE walls with metallic reinforcements, which was independent of the design guidelines provided by vendors of proprietary MSE wall systems. FHWA (1987) provided guidance on accounting for reinforcement durability and corrosion resistance in design to achieve a design life of 75 years for conventional structures and 100 years for critical structures. This guidance recommended using reinforcement which included sacrificial steel to account for the loss of base metal due to corrosion. The recommended thickness of the sacrificial steel, based on the assumption of constant corrosion rate with time, was 0.03 in. and 0.05 in. for permanent and critical permanent structures respectively. FHWA (1987) also raised awareness about the importance of proper drainage design to avoid saturation or interception of reinforced fills with flows carrying corrosive deicing salts.

Overall, there are numerous studies and publications that contributed to the evolution of the state-of-the-practice of MSE walls (e.g., Christopher et al. 1989a, 1989b; Mitchell and Villet 1987; Elias and Christopher 1996; Elias et al. 2001; Berg et al. 2009a, 2009b). The next section will summarize some of the developments that have been incorporated into the current state-of-the-practice, as compared to early practice.

2.1 Evolution of Reinforcement Specifications

Consideration of time-dependent degradation of structural metallic components (reinforcements and facing connections) is essential in the prediction of the remaining service life of aging MSE walls. While early practice did not consider design life, FHWA (1987) specified a target design life of 75 years for conventional structures and 100 years for critical ones. Additionally, the

specifications provided by FHWA (1985) introduced a change to steel type and strength, which increased from Grade 40 to Grade 65. In contrast to current practice that requires the use of galvanization for corrosion protection, early practice up until the mid-1980s involved the use of fusion bonded epoxy by transportation agencies in some MSE structures. However, the use of epoxy was found ineffective for corrosion protection (Elias et al. 2001). Specification for the galvanized coating thickness changed from approximately 48 microns, generally adopted in early practice, to 86 microns (2 oz/sf) in current practice. This change is believed to have taken place with the launch of the FHWA MSE design specifications by Christopher et al. (1989a, 1989b) and Elias (1990). Table 1 shows the evolution in the recommended properties for reinforcement used in MSE walls.

2.2 Evolution of Reinforced Fill Specifications

Specifications for reinforced fill materials have evolved to ensure that such materials have suitable electrochemical properties to alleviate the potential for reinforcement degradation by corrosion. In current practice (Berg et al. 2009a, 2009b; AASHTO 2020), suitable reinforced fills are materials that have a minimum soil resistivity greater than 3000 ohm-cm, a pH value between 5 and 10, chloride content less than 100 ppm, sulfate content less than 200 ppm, and organic content less than 1%. These guidelines were developed based on numerous studies by multiple investigators. For example, an early study by Darbin et al. (1979) investigated the effect of soil electrochemical properties on corrosion and indicated that chloride contents of up to 200 ppm and sulfate contents of up to 1000 ppm have no significant effect on corrosion rate. A subsequent study by Terre Armee Internationale (1982) provided a summary of the soil electrochemical properties of several of non-marine MSE walls, finding that 98% had resistivities greater than 1000 ohm-cm, 98% had pH values ranging from 5 to 9.5, 98% had chloride contents less than 200 ppm, and 97% had sulfate contents less than 1000 ppm (after Mitchell and Villet 1987). This information indicates that a considerable number of MSE walls constructed in the 1970s and early 1980s used reinforced fills that may not comply with the current specifications. Specifications have been developed based on soil electrochemical characterization tests for resistivity, pH value, sulfate content, and chloride content, as shown in Table 2. Additionally, the use of well-graded select reinforced fills with fines content less than 15% has been recommended (FHWA 1987) to promote drainage and ease of construction, a change from guidance adopted in the 1970s and early 1980s where fills with fines contents up to 25% were recommended.

Table 1. Evolution of Design Specifications on Metallic Reinforcement

Reference	Year	Reinforcement	Galvanization	Coating Thickness	Design Corrosion Rate
FHWA Specs	1974	ASTM A446 Grade C	ASTM A525 Class G210	-	-
Chang et al.	1974	-	-	-	-
FHWA Specs	1979	ASTM A36 + ASTM A570 Grade C	ASTM A123	-	-
FHWA Specs	1985	AASHTO M223 Grade 65	AASHTO M111	-	-
Mitchell and Villet	1987	-	-	Galvanization: 3.4 mils	Zinc: 6 µm/yr for the first 2 years then 2 µm/yr Carbon steel: 45 µm/yr after zinc depletion[c]
FHWA Guide	1987	-	AASHTO M111	-	-
Christopher et al. Vol. 1 and 2	1989	-	ASTM A123	Galvanization: 3.4 mils Resin-Bonded Epoxy: 18 mils	-
AASTHO	1990	ASTM A36 or ASTM A572 Grade 65	AASHTO M111 (ASTM A123)	-	-
AASTHO	1991	AASHTO M223 (ASTM A572) Grade 65	AASHTO M111[a]	Resin-Bonded Epoxy: 16 mils	Zinc: 15 µm/yr for the first 2 years then 4 µm/yr Carbon steel: 15 µm/yr after zinc depletion
FHWA Specs	1992	AASHTO M223 Grade 65 Type 3	AASHTO M111	-	Zinc: 15 µm/yr for the first 2 years then 4 µm/yr Carbon steel: 12 µm/yr after zinc depletion
Elias and Christopher	1997	ASTM A-36 or ASTM A-572 Grade 65 (AASHTO M-223)	AASHTO M111 (ASTM A123)	-	Zinc: 15 µm/yr for the first 2 years then 4 µm/yr Carbon steel: 12 µm/yr after zinc depletion
Elias et al.	2001	ASTM A-36 or ASTM A-572 Grade 65 (AASHTO M-223)	AASHTO M111 (ASTM A123)	Galvanization: 3.4 mils	Zinc: 15 µm/yr for the first 2 years then 4 µm/yr Carbon steel: 12 µm/yr after zinc depletion
Berg et al. Vol. 1 and 2	2009	ASTM A572 Grade 65	AASHTO M111 (ASTM A123)[a]	Galvanization: 3.4-3.9 mils[b] Resin-Bonded Epoxy: 18 mils	Zinc: 15 µm/yr for the first 2 years then 4 µm/yr Carbon steel: 12 µm/yr after zinc depletion
Taylor et al.	2023	ASTM A572 or ASTM A1011 (strips) ASTM A1064 (wire grids)	ASTM A123	Galvanization: 3.4 mils (3.9 mils for strips with thicknesses > ¼")	Zinc: 15 µm/yr for the first 2 years then 4 µm/yr Carbon steel: 12 µm/yr after zinc depletion

(1) "-" denotes information not available.

(2) [a] Corrosion-resistant coating can be used in lieu of galvanization and shall be electrostatically applied.

(3) [b] Minimum galvanization thickness is 3.4 mils for wire meshes and bar mats of all sizes, and steep strips with thicknesses < ¼", and is 3.9 mils for strips with thicknesses > ¼".

(4) [c] Carbon steel corrosion rate for the first 2 years and normal backfill condition. Mitchell and Villet (1987) provided corrosion rates for following years depending on soil resistivity. Corrosion rates were also provided for saline environments.

After Govindasamy et al. 2018.

Table 2. Evolution of Design Specifications on Reinforced Fill

Reference	Year	D_{max} (in.)	FC (%)	PI (%)	ϕ (deg)	ρ_{min} (Ω.cm)		pH		Chloride Content (ppm)		Sulfate Content (ppm)		RC (%)	
		Range	Range	Range	Range	Range	Method	Range	Method	Range	Method	Range	Method	Range	Method
FHWA Specs	1974	<4	<15	-	>25	-	-	-	-	-	-	-	-	-	-
Walkinshaw	1975	-	<25	-	-	-	-	-	-	-	-	-	-	-	-
FHWA Specs	1985	<3	<25[a]	-	-	>3000	-	5–10	-	<200	-	<1000	-	-	
Mitchell and Villet	1987	<6	<25[a]	-	-	>1000	-	4.5–9.5	-	<200[b]	-	<1000	-	-	-
FHWA Guide	1987	<4	<15	<6	-	>3000	California DOT 643	5–10	California DOT 643	<50	California DOT 422	<500	California DOT 417	-	-
Christopher et al. Vol. 1 & 2	1989	<4	<15	<6	-	>3000	California DOT 643	5–10	California DOT 643	<200	California DOT 422	<1000	California DOT 417	95	AASHTO T99
AASTHO	1990	<4	<15	<6	>34	>3000	California DOT 643	5–10	California DOT 643	<100	California DOT 422	<200	California DOT 417	-	-
AASTHO	1991	<4	<15	<6	>34	>3000	California DOT 643	5–10	California DOT 643	<50	California DOT 422	<500	California DOT 417	95	AASHTO T99
FHWA Specs	1992	<3	<15	<6	>34	>3000	AASHTO T288	5–10	AASHTO T289	<200	AASHTO T291	<1000	AASHTO T290	-	-
Elias and Christopher	1997	<4	<15	<6	-	>3000	AASHTO T288	5–10	AASHTO T289	<100	AASHTO T291	<200	AASHTO T290	95	AASHTO T99
Elias et al.	2001	<4	<15	<6	-	>3000	AASHTO T288	5–10	AASHTO T289	<100	AASHTO T291	<200	AASHTO T290	95	AASHTO T99
Berg et al. Vol. 1 and 2	2009	<4	<15	<6	>34	>3000	AASHTO T288	5–10	AASHTO T289	<100	ASTM D4327	<200	ASTM D4327	95	AASHTO T99 or T180
Taylor et al.	2023	<4	<15	<6	>34	>3000	AASHTO T288	5–10	AASHTO T289	<100	AASHTO T291	<200	AASHTO T290	95	AASHTO T99

(1) "-" denotes information not available.
(2) [a] For backfill materials with FC > 15%, the fraction of particles with D < 15 μm shall not exceed 15% and ϕ shall not be less than 34 deg.
(3) [b] Except when dealing with deicing salts.
(4) The heading "Range" in the table refers to the specified range of properties.
(5) The heading "Method" refers to the relevant test method for the property.
(6) The definitions of the symbols and abbreviations in the table are as follows: D_{max}: Maximum Particle Size; FC: Fines Content; PI: Plasticity Index; ρ_{min}: Minimum Resistivity; RC: Relative Compaction.

After Govindasamy et al. 2018.

3. Deterioration of Reinforced Soil Walls

The performance of reinforced soil wall assets degrades due to deterioration processes that occur to their constituting elements, including fills, reinforcements, facings, and drainage systems. Each element degrades through a number of deterioration mechanisms that contribute variably to the overall deterioration of the asset.

3.1 Reinforcement degradation

Reinforcements used in reinforced soil structures are often metallic or polymeric, both of which are prone to progressive deterioration (Elias et al. 2009). The early generations of MSE walls were constructed using metallic reinforcements, which deteriorate primarily due to corrosion at continuously varying rates. While significant research has been conducted to study the corrosion of steel buried in soils, corrosion remains a significant challenge in the asset management of MSE walls for its high uncertainty and variability, both spatially and temporally. Cumulative corrosion of buried steel has typically been estimated as a function of time using a power law, as follows:

$$X = K.t^m$$

where X is the average corrosion thickness loss, K is a coefficient that depends on soil corrosivity, t is the time, m is a time exponent (Romanoff 1956; Bastick and Jallioux 1992; Elias et al. 2009; Fishman and Withiam 2011; NASEM 2023). A number of predictive models were developed to evaluate the corrosion of buried steel, especially in MSE walls (Fishman and Withiam 2011), as presented in Table 3. These models were developed to be used in the design of MSE walls and are deemed overly conservative to account for the uncertainties associated with corrosion and its progression with time. However, it may be impractical to use such overly conservative models for the evaluation of reinforcement corrosion in existing MSE walls, which have been built since the 1970s, for asset management purposes. Moreover, current corrosion models were developed to provide predictions of reinforcement corrosion as a function of time for fills having characteristics that are deemed mildly corrosive and drainable. Fills used in early MSE wall generations may not have the characteristics that meet the criteria for mildly corrosive and drainable fills used in the development of these predictive models.

Table 3. Corrosion Predictive Models

Model	Steel Type	Equation (1)
Darbin Model (Darbin et al. 1988)	Galvanized	$X = 50 \times t_f^{0.65} - 2 \times z_i$ for $t_f > \left(\frac{z_i}{25}\right)^{1.54}$ $X = 0$ for $t_f > \left(\frac{z_i}{25}\right)^{1.54}$
Elias (1990)	Plain Steel	$X = 80 \times t_f^{0.80}$
Stuttgart Model (Rehm 1980) Low Salt Content	Galvanized	$X = 9\left(t_f - 2 - \frac{z_i - 12}{2}\right)$
	Plain Steel	$X = 90 + 9(t_f - 2)$
Stuttgart Model (Rehm 1980) High Salt Content	Galvanized	$X = 12\left(t_f - 3 - \frac{z_i - 51}{2}\right)$
	Plain Steel	$X = 160 + 12(t_f - 2)$
AASHTO Model	General	$X = 12\left(t_f - 2 - \frac{z_i - 30}{4}\right)$
Caltrans Model	General	$X = K(t_f - C_{yrs})$ K and C_{yrs} are constants that depend on soil type.

(1) X is corrosion thickness loss in mm; z_i is zinc depletion in mm; and t_f is time in years.

Corrosion rates are governed by the electrical conductivity of the fill in which the reinforcements are placed (Nicks et al. 2017; Bronson et al. 2020; Kolay et al. 2020). The electrical conductivity primarily depends on fill moisture, concentration of soluble salts (chlorides and sulfates), and pH value (Elias et al. 2009). This is typically accounted for in design by using galvanized reinforcements and connections to delay steel corrosion. Additionally, cross-sections of reinforcement and connections are designed to include sacrificial steel thickness. The key factors governing corrosion rates can be summarized as follows: (1) soil moisture content; (2) soil resistivity; (3) pH value; (4) chlorides and sulfates contents; (5) presence of anaerobic bacteria; (6) soil temperature; and (7) soil aeration.

3.1.1 Soil moisture content

Soil moisture content is a key element for corrosion of buried metals as it forms the electrolyte necessary for the corrosion-related chemical reactions to take place. Corrosion rate increases with increasing moisture content up to a critical level beyond which corrosion rate decreases with further increasing moisture content (Gupta and Gupta 1979; Noor and Al-Moubarki 2014; Wasim et al. 2018; Ezuber et al. 2021; Liu et al. 2023), as shown in Figure 1a, due to the decrease in the air content. The critical moisture content was found to range from 10 to 30% based on several studies

consulted herein that involved a range of soils, as shown in Figure 1b. Gupta and Gupta (1979) reported that the critical moisture content can be approximated to 65% of the soil water holding capacity.

Figure 1. Effect Of Soil Moisture Content on Corrosion Rate: (A) Idealized Relationship; and (B) Data Reported in the Literature

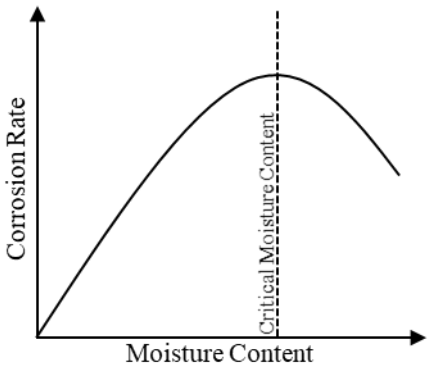

(a)

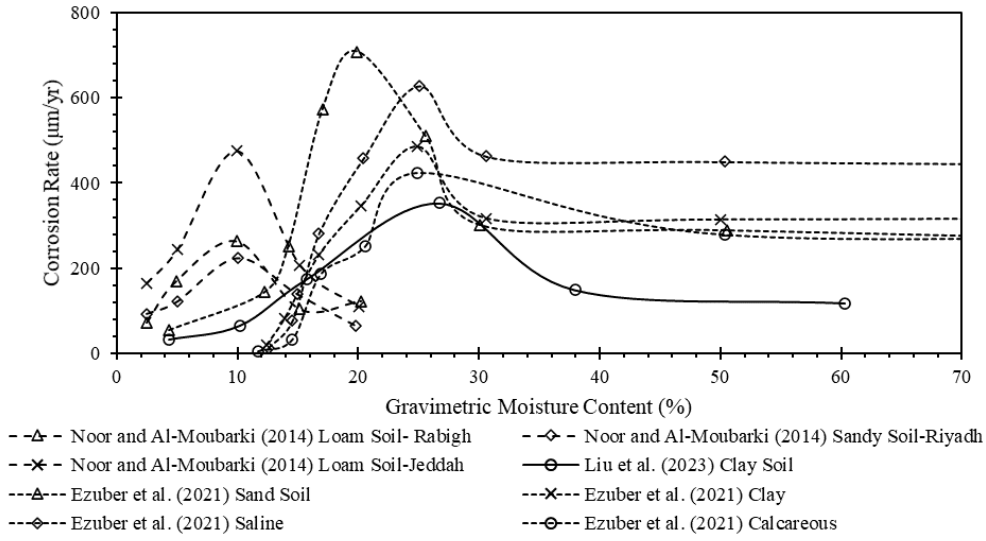

(b)

3.1.2 Soil resistivity

Soil resistivity is the reciprocal of soil conductivity and has a direct relationship with the electrical currents generated in the corrosion reactions. Soil resistivity can be evaluated in the lab through an index test that measures the minimum soil resistivity according to an AASHTO test standard (AASHTO T 288). The minimum soil resistivity obtained experimentally is indicative of soil corrosivity and can be used as a metric, along with other metrics, to evaluate soil corrosivity in practice. The relationship between soil resistivity and corrosion rate can generally be represented as shown in Figure 2a. Data of soil resistivity and corresponding corrosion rate reported by Romanoff (1956) and Fishman and Withiam (2011) are shown in Figure 2b.

Figure 2. Effect of Soil Resistivity on Corrosion Rate: (A) Idealized Relationship; and (B) Data Reported in the Literature

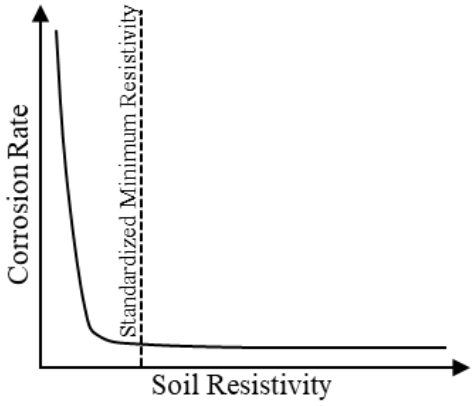

(a)

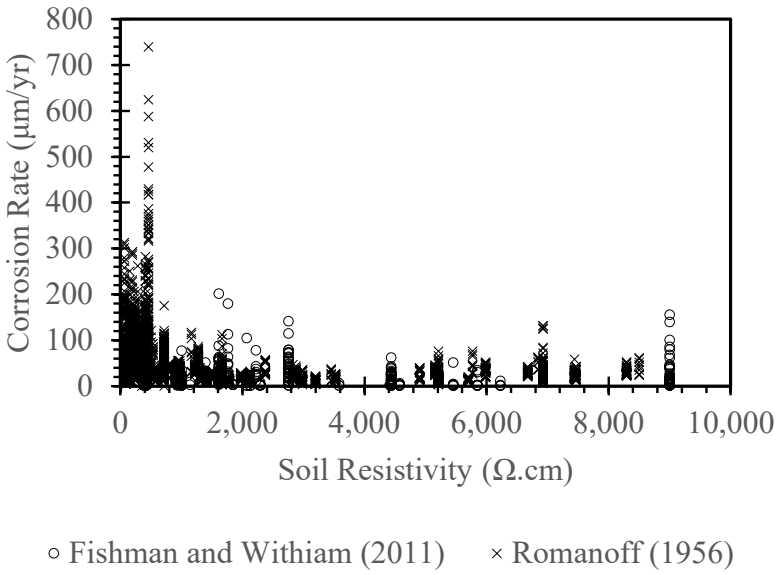

(b)

A direct relationship between soil resistivity and moisture content had been proposed by Archie (1942) and developed by Waxman and Smits (1968). The relationship correlates soil resistivity with the cation exchange capacity, CEC, of the soil particles. Generally, coarse-grained soils with high hydraulic conductivity can be free draining and may not easily retain water at the steel surface, whereas fine-grained soils with low hydraulic conductivity may retain water at the steel surface (NASEM 2023). Drainage in soils is dominated by the smaller grain fraction that fills the space between larger grains introducing small-diameter pore networks, which tend to retain moisture through capillary action (NASEM 2023). Since early wall generations could have a fines content of up to 25% (see Table 2), it is appropriate to consider CEC in evaluating the resistivity of reinforced fills used in early-generation MSE walls. Table 4 summarizes CEC ranges reported by Kennedy (1965) for various soil types and regions. The relationship proposed by Waxman and Smits (1968) was modified by Chambers et al. (2014), where the soil resistivity can be expressed as follows:

$$\rho = \frac{F.\left[\frac{n}{(1-n).G_s.w}\right]^{\beta}}{\frac{1}{\rho_w} + \left(\frac{B.CEC}{100.w}\right)\left(\frac{\gamma_w}{g}\right)}$$

where ρ is the soil resistivity in Ω.m; F is a formation factor and can be taken as $1/n^2$ (Archie 1942; Worthington 1993); n is soil porosity; β is saturation exponent and can be taken as 2.0 in the absence of data (Telford et al. 1991); w is the gravimetric water content; CEC is the cation exchange capacity in meq/100g and was taken as 5.5 meq/100g (as an example for low plasticity fines); G_s is the specific gravity and was taken as 2.7; B is the average mobility of cations and was taken as 2.04 cm3/meq/ Ω.m (Merrit et al. 2016); ρ_w is the pore water conductivity and was taken as 10.13 Ω.m (Merrit et al. 2016); γ_w is the unit weight of water; and g is the gravitational acceleration.

Table 4. Typical CEC Values of Different Soil Types in the US

Material	Region	CEC Range (meq/100g)
Clay-size fractions	Eastern US	14–28
Clay-size fractions	Central and West-Central US	25–65
Clay-size fractions	California and Oregon	18–65
Sand	General	0.3–13
Silt	General	4–30

Data From Kennedy 1965.

3.1.3 pH value

pH value contributes to the progression of corrosion. As shown in Figure 3, corrosion rates have been reported to generally decrease with increasing pH values in acidic environments (pH values < 7) and increase with increasing pH values in alkaline environments (pH values > 7) (Rossum 1969; Mughabghab and Sullivan 1989). Corrosion progression is generally high in neutral and acidic environments (Shreir et al. 1994; Roberge 2000). Corrosion progression slows down at relatively high pH values where metal oxides are stable because the spontaneous formation of the oxides can provide protection (in the form of rust scales) to the underlying metal (NASEM 2023). Mughabghab and Sullivan (1989) proposed a model for the coefficient K based on the data of Romanoff (1956), which can be expressed as follows:

$$K = \begin{cases} 5.74 \times (9.87 - pH), & for\ acidic\ soils \\ 5.05 \times (2pH - 10.26), & for\ alkaline\ soils \end{cases}$$

Figure 3. Effect of pH Value on Corrosion Rate: (A) Idealized Relationship; and (B) Data Reported in the Literature

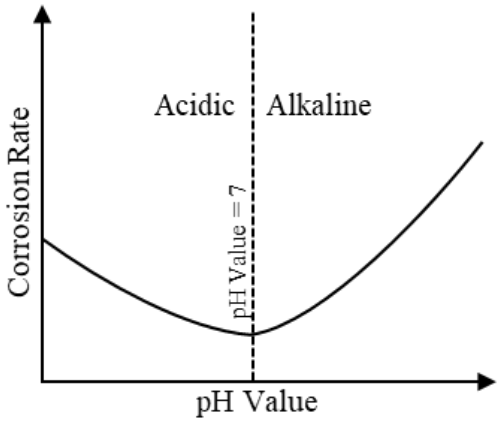

(a)

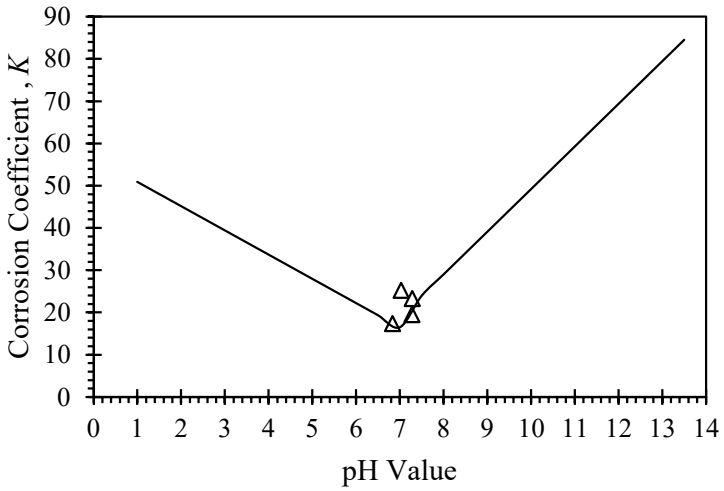

(b)

Source: Mughabghab and Sullivan 1989.

3.1.4 Chloride and sulfate contents

Corrosion rates increase with increasing soil salt content (Romanoff 1956; Bastick and Jailloux 1992). Ions of chloride and sulfate salts are particularly classified as aggressively corrosive ions. Chlorides destroy the protective rust layers of metals, exposing the underlying metal to further corrosion. Sulfates are considered less corrosive compared to chlorides unless anaerobic sulfate-reducing bacteria exist. Bastick and Jailloux (1992) reported that chlorides and sulfates have similar effects on corrosion rates up to concentrations of 100 ppm. For concentrations higher than 100

ppm, the effect of chlorides on corrosion rates become much high than that of sulfates, as shown in Figure 4. Bastick and Jailloux (1992) proposed a model for the coefficient K that can be expressed as follows:

$$K = 0.21 \times [Cl^-]^{0.86} + 2.74 \times \left[{SO_4}^{2-}\right]^{0.32}$$

where Cl^- and ${SO_4}^{2-}$ are the chlorides and sulfates concentrations in ppm.

Figure 4. Effect of Chlorides and Sulfates on Corrosion Rate: (A) Idealized Relationship; and (B) Data Reported in the Literature

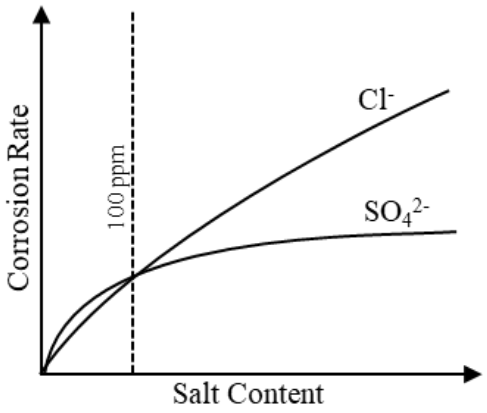

(a)

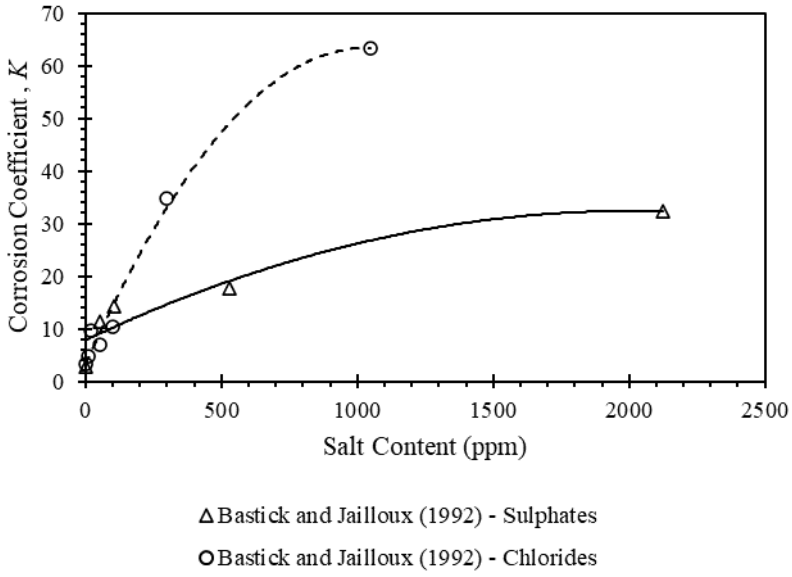

(b)

3.1.5 Presence of anaerobic bacteria

The presence of microorganisms contributes to metal corrosion (Costerton et al. 1987; Hubert et al. 2005; Enning et al. 2012). The bacterial metabolism, reproduction, and growth occur through microbiological activities, forming a biofilm that may degrade metals (Hamilton 1985). Organic content is generally restricted to 1% for fills used in MSE walls.

3.1.6 Soil temperature

Corrosion rate generally increases with increasing temperature up to a critical level beyond which the corrosion rate decreases with increasing temperature due to the decrease in oxygen solubility in water (Davalos et al. 1992; NASEM 2023). The maximum corrosion rate was reported to be at 70°C (NASEM 2023). Figure 5 illustrates the effect of soil temperature on corrosion rate.

Figure 5. Effect of Temperature on Corrosion Rate: (A) Idealized Relationship Between Soil Temperature and Corrosion Rate; and (B) Data Reported in the Literature for Ambient Temperature and Corrosion Rate

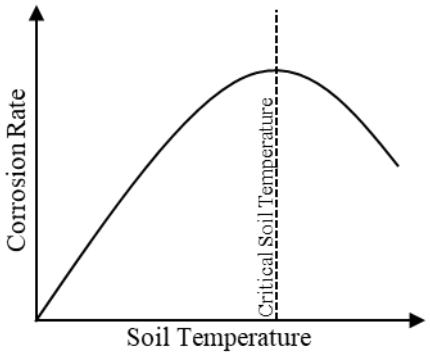

(a)

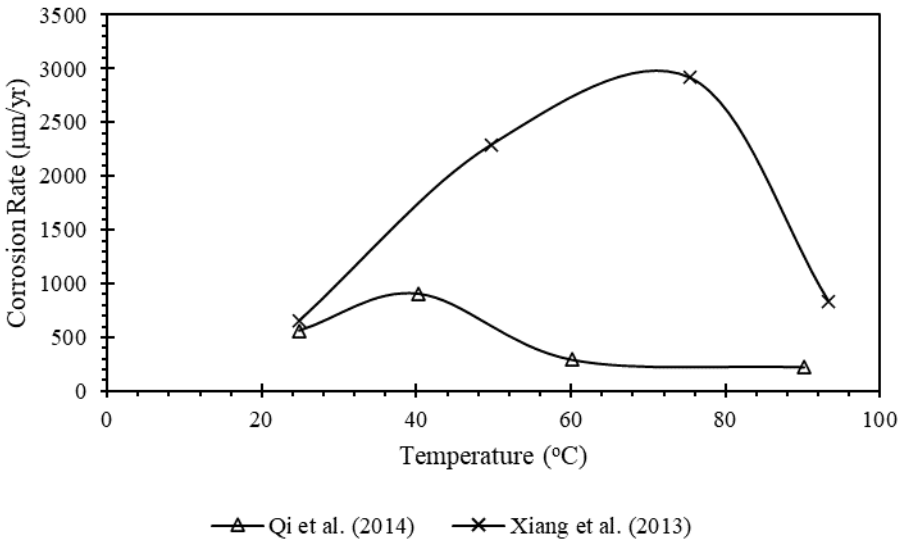

(b)

3.1.7 Soil aeration

Soil aeration has been identified as a contributing factor to corrosion of buried metals (Romanoff 1956). Soil aeration provides an oxygen supply that contributes to corrosion. According to Rossum (1969), the first model of soil corrosion was based on electrochemical principles of pitting corrosion in steel. Four types of soil aeration were proposed: (1) well aerated soils; (2) fairly aerated soils; (3) poorly aerated soils; and (4) very poorly aerated soils. Figure 6 and Table 5 present the difference in pit-depth which is considered as corrosion growth:

Table 5. Corrosion Pit Depth Based on Soil Aeration

Soil Type	Corrosion Pit Depth
Well aerated soils	$P = (6K)^{1/6} \times t^{1/6}$
Fairly aerated soils	$P = (K)^{1/3} \times i_o \times t^{1/3}$
Poorly aerated soils	$P = K \times t^{1/2}$
Very poorly aerated soils	$P = K \times t^{2/3}$
***P* is pitting corrosion depth, *K* is corrosion coefficient, *t* is time, and i_o is initial current per pit.**	

After Rossum 1969.

Figure 6. Effect of Soil Aeration on Corrosion Rate

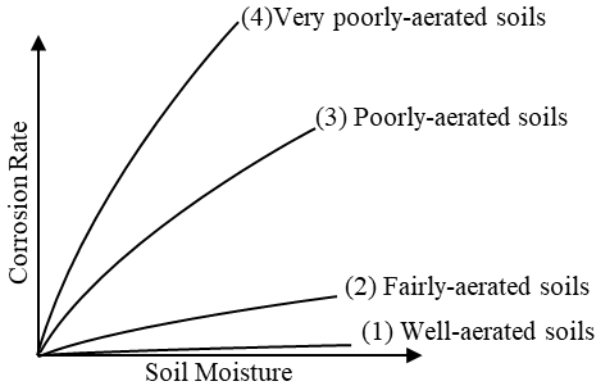

3.2 Reinforced Fill Degradation

Reinforced fills can cause reinforcement corrosion if they have a large salt content or a high ability to hold water (i.e., fills with low permeability) as either can create a wet environment with low electrical resistivity that exacerbates reinforcement corrosion. As walls age, salt content in fills may increase where deicing chemicals are frequently applied, especially in walls constructed with no surface drainage systems (Govindasamy et al. 2018). Additionally, fills in reinforced soil walls may be prone to internal erosion by suffusion and induced settlement (Sibille et al. 2015; Breckwoldt et al. 2019), which in turn lead to localized stress concentrations in the reinforcements and overall

deterioration in the asset performance. Cycles of weather-driven wetting and drying can promote migration of fines through granular reinforced fills (Breckwoldt et al. 2019). This migration of fines may lead to fines accumulation near the base of the reinforced fill and clog the drainage system, which can increase the moisture content in the reinforced fill and accelerate reinforcement corrosion (Breckwoldt et al. 2019; Taylor et al. 2023). Granular fills may also creep with time due to interparticle sliding and delayed crushability of particles (Bowman and Soga 2003; Kwok and Bolton 2013; Liu et al. 2019; Gavin and Igoe 2021; Liu et al. 2022).

3.3 Drainage Systems Degradation

Drainage systems in current practice include surface drainage, subsurface drainage, and salt intrusion protection systems. Poor surface drainage or the absence of a proper salt intrusion system can cause infiltration of water into the reinforced fill. This water infiltration can be accompanied by salt intrusion where deicing salts are applied. This can lead to an increase in the moisture and salt content in the reinforced fill, especially if the fill material has low permeability or if the subsurface drainage system is inadequately removing the infiltrated water. The increased moisture and salt content accelerate the corrosion of metallic reinforcements and facing connections. Poor subsurface drainage can cause water to accumulate and infilitrate into the reinforced fill, either from the surface of the wall or from the retained backfill (Govindsamy et al. 2018), which can lead to increased stresses on the reinforcements and facing connections.

4. Asset Management Practices

Earth retaining structures are key features in many civil engineering projects. They are often categorized by their functions and types. Main categories include externally stabilized fill walls, internally stabilized fill walls, externally stabilized cut walls, and internally stabilized cut walls (Sabatini et al. 1999). Individual walls may not be large or expensive, but they collectively constitute an important asset that can be difficult to manage due to the dispersed nature of wall assets, the different types of wall construction, and the different purposes walls serve (Anderson et al. 2009). Retaining walls are an integral component of the National Highway System infrastructure that should be incorporated into its master planning, rehabilitation, maintenance, and asset management (Gabr et al. 2017). While transportation agencies have long focused on the expansion of roads, bridges, and other transportation infrastructure assets, attention has shifted away from the development of new infrastructures to intelligently maintaining existing assets due to the impacts of budget shortages and growing demand (Arif and Bayraktar 2012).

A significant limitation of current asset management systems is the lack of consideration of geotechnical assets (Sanford Bernhardt et al. 2003). Sanford Bernhardt et al. (2003) provided a framework for managing geotechnical features using asset management principles. The framework was based on a generic framework proposed by the FHWA that considers the unique aspects of geotechnical features. As per the Moving Ahead for Progress in the 21st Century Act (MAP-21 2012), state highway agencies are required to "develop a risk-based asset management plan for the National Highway System to improve or preserve the condition of the assets and the performance of the system, including signs and sign structures, earth retaining walls and drainage structures." Later, Vessely et al. (2019a, 2019b) developed an implementation manual for geotechnical asset management for transportation agencies, which was published in NCHRP Report 903.

Several experts in MSE walls have recently presented methods to help infrastructure stakeholders develop their own MSE asset management methods (Adams and Nicks 2017; DiMaggio and MacMillan 2018; Govindasamy et al. 2018). Adams and Nicks (2017) argued that the assessment of MSE walls should manage the effects of uncertainty and poor practice that pertain to the main drives of MSE wall failures, which include soil type, design, communication, water, and construction. Tarawneh et al. (2017) implemented a large-scale inspection program to identify the most frequent MSE wall problems. They proposed an inspection rating system and a risk assessment method to determine the overall rating of an MSE wall. Govindasamy et al. (2018) developed a risk-based protocol for asset management of MSE walls with metallic reinforcements. They based their assessment on a qualitative fault tree analysis that tracks the causes of failure due to corrosion.

Butler et al. (2016) developed a retaining wall information collection and assessment system (WICAS) to readily collect data in the field that involved a two-part condition assessment model. That model provides a rating of the retaining wall condition as well as the potential problems with

specific wall components, which may be overlooked through the presentation of an overall wall average rating. DiMaggio and MacMillan (2018) proposed a systematic approach for asset management of reinforced soil walls that includes (1) developing an inventory specifically for reinforced soil walls, ideally using a GIS platform to keep track of the existing assets and their geographical locations in an organized digital fashion; (2) defining pertinent limit states and behavioral mechanisms that can be used to develop performance variables that are integratable within an inspection protocol; and (3) developing an inspection protocol that involves condition assessment, routine inspection, and data storage and interpretation. For the condition assessment, they suggested developing a baseline condition based on a rating of vulnerability. Several infrastructure stakeholders have developed or are developing methods to create an inventory for their MSE wall assets, either in a separate inventory or as part of larger inventories that serve all retaining walls in their respective ownership (Gerber 2012; Zekkos et al. 2020). Walls are typically admitted to inventories according to criteria based on wall attributes, such as exposed height, retained earth height, wall length, face slope, wall batter, location relative to roadways, relation to other assets (e.g., bridges, culverts), and wall ownership (Brutus and Tauber 2009; Gerber 2012; Zekkos et al. 2020). Table 6 summarizes retaining wall admission criteria for inventories and inspection frequency.

Table 6. Summary of Retaining Wall Admission Criteria to Inventories and Inspection Frequency

Agency	Year of Inventory	Height (ft.)	Wall Face Angle (deg)	Distance from Abutment (ft.)	Inspection Frequency (yr.)
National Parks Service (NPS)	2010	> 4	> 45	> 40	10
Alaska DOT	2013	> 4	> 45	> 100	5
Colorado DOT	2016	> 4	> 45	> 40	6
North Carolina DOT	2015	-	-	-	-
Pennsylvania DOT	2010	-	-	> 100	5
Nebraska DOR	2009	-	-	-	-
New York City DOT	1998	> 6	-	-	5
New York State DOT	2015	> 6	> 33	> 33	-
Wisconsin DOT	2011	> 5	-	-	6
Oregon DOT	2007	> 4	-	-	5
Utah DOT	2009	-	-	-	-
Ohio DOT	2007	-	-	-	-
City of Cincinnati	1990	> 2	-	-	6
City of Seattle	2009	-	-	-	4

After Zekkos Et Al. 2020.

For inventoried walls, routine inspections are typically performed every two to ten years, with the most common interval being five years. Walls that perform poorly or are in an environmentally adverse situation may require inspection more often. Inspection includes observations of any wall tilt, bulge, misalignment of joints, cracking, spalling, settlement, rust staining, vegetation, and drainage issues (Brutus and Tauber 2009; Gerber 2012; Govindasamy et al. 2015; Zekkos et al. 2020). Table 7 summarizes the techniques and procedures used by various state agencies in monitoring their retaining walls. California has been the leading state in corrosion monitoring in MSE walls since 1987, with inspection intervals set at five to ten years. The state has introduced inspection elements into new constructions, and tensile strength tests have been carried out on extracted elements. In addition, electrochemical, linear polarization resistance (LPR), and electrochemical impedance spectroscopy (EIS) tests have also been part of the California corrosion monitoring program (Fishman and Withiam 2011).

Table 7. Monitoring Techniques and Procedures For Retaining Walls

State	Monitoring Techniques and Procedures
California	• Regular visual inspections to identify visible signs of distress. • Advanced condition assessments using LiDAR for topographical analysis. • Corrosion monitoring via coupon testing, half-cell potential measurements, and linear polarization resistance to assess and predict corrosion rates. Specimens are prepared following ASTM G1-03.
Texas	• Manual inspections complemented by non-destructive testing methods to assess the structural integrity without causing damage. • Installation of strain gauges and tilt meters to monitor changes in stresses and displacements within wall components.
Missouri	• Biennial visual inspections coupled with instrument-based assessments to monitor wall conditions, including alignment and corrosion. • Use of ground penetrating radar (GPR) and photogrammetry to provide a detailed condition assessment, identifying subsurface anomalies and surface changes.
Nebraska	• Triennial inspections focusing on structural integrity and corrosion, utilizing visual and instrument-based techniques. • Use of piezometers and strain gauges to measure physical changes and stresses, providing data necessary for proactive maintenance decision making.
Pennsylvania	• A combination of visual inspections and instrument-based monitoring. • Utilization of slope indicators, crack gauges, and tilt meters for real-time monitoring of displacements and straining. • LiDAR and photogrammetry are employed for precise surface condition assessment, aiding in the early detection of potential issues. • Regular corrosion monitoring.

Information in this table was synthesized from Elias et al. 2009; Fishman and Withiam 2011; Gerber 2012; Zekkos et al. 2020.

Despite the growing efforts to develop and improve asset management practices for MSE walls, several challenges remain. The absence of standardized guidelines and protocols stands out as a significant issue, necessitating unifying efforts to develop national or regional directives that offer clear instructions on asset management tailored specifically to MSE walls. Additionally, current practices rely on infrequent physical inspections, if any, and on reporting signs of potential deterioration. While these inspections are valuable and noting signs of deterioration can be indicative of developing distress in MSE walls, they fall short of providing quantitative estimates of stability and remaining service life. For instance, Gabr et al. (2017) used field survey results from earth retaining structures, including MSE walls among others, to illustrate the disadvantages of rating systems that solely provide an overall wall average rating.

5. Reinforced Soil Wall Computer Model

This study focused on the deterioration of metallically reinforced MSE walls due to corrosion, as this is considered the main deterioration mechanism in such walls. This section presents a framework for the development of an asset-scale hydromechanical MSE wall model that incorporates material-scale deterioration. The numerical model was developed as a representative example of early-generation MSE walls constructed in the 1970s. The characteristics of this hypothetical wall were assumed to follow the specifications available in the 1970s (see Table 1 and Table 2) and the specifications used in the construction of two failure case studies in Westchester County, NY, which were constructed between 1977 and 1979 and failed in October 2016 (NYSDOT 2016). These walls underwent an extensive investigation program after their failure. Where applicable, data from these walls were used to showcase the purpose of the numerical model developed in this study.

The numerical model involved reinforced fill, reinforcing inclusions, wall facing, retained fill, and embedment fill. The height of the exemplar wall was assumed to be 6.0 m. Reinforcements were assumed to be smooth steel strips spaced at 0.75 m in both the vertical and horizontal directions. Facing was assumed to be 1.5 m × 1.5 m segmental concrete panels that are 0.15 m in thickness and inclined at 1H:16V. The reinforced fill was assumed to have been constructed in lifts 0.25 m in thickness simultaneously with the retained fill. The embedment fill placed in front of the wall was taken as 0.5 m or 5% of the wall height, whichever is larger. The wall was modeled with no drainage systems.

5.1 Model Description

FLAC (Fast Lagrangian Analysis of Continua) code was used to develop the model in a plane-strain condition and considered the multi-phase hydromechanical behavior of the wall. The code uses an explicit finite difference method to perform numerical computations of grided models for geotechnical engineering applications (Itasca 2019). The size of the mesh zones was selected to be equivalent to half the typical thickness of fill lift layers to facilitate the simulation of the construction sequence. The selected mesh zone size (0.125 m × 0.125 m) is deemed small enough to minimize mesh dependency and render accurate results for both mechanical and hydraulic responses of MSE walls.

5.2 Boundary Conditions

The wall was assumed to rest on competent rock, and the model bottom boundary was accordingly fixed in both the horizontal and vertical directions. The lateral boundaries were constrained from displacement in the horizontal direction and were allowed to displace freely in the vertical direction. The lateral extents from the face and the back of the wall were selected to be equivalent to the wall height, as shown in Figure 7. Since the purpose of the model is to predict the variation

of moisture and stresses within the reinforced fill, these boundaries were considered reasonable, especially for such computationally expensive models. Flow was restricted through the model side and bottom boundaries, which allowed for free pore pressure changes over time.

Figure 7. Finite-Difference Mesh Used to Model the Exemplar Reinforced Soil Wall (H = 6 m)

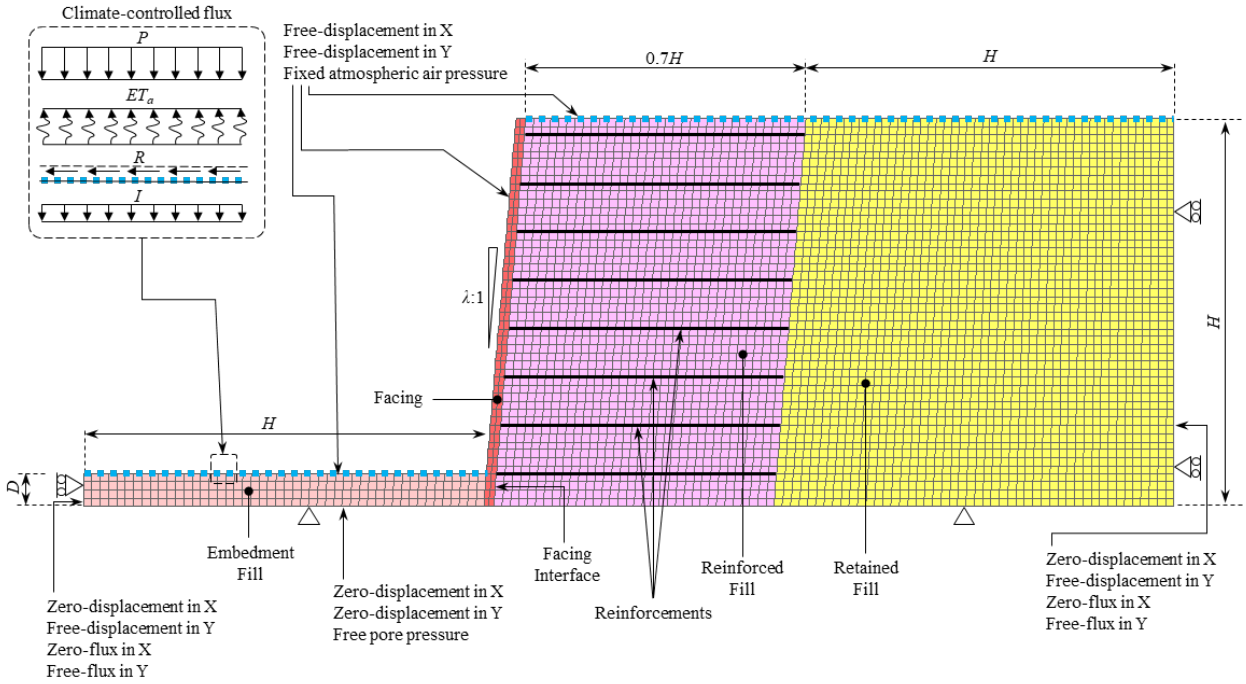

To simulate climate effects, a transient climate boundary was defined at the surface of the model that updates at one-simulation-hour intervals. The climate boundary calculates the daily surface net flux, q_{nf}, as the difference between precipitation, P, and potential evapotranspiration, ET_o. By way of example, weather parameters were obtained from weather stations local to the Westchester County case study walls (downloaded from NOAA) between 1977 and 2016 to estimate potential evapotranspiration, ET_o, using the Penman-Monteith method as adopted by FAO56 (Allen et al. 1998). Detailed descriptions of the implementation of the climate boundary can be found in Morsy et al. (2023). Figure 8 presents the annual cumulative precipitation and annual cumulative actual evapotranspiration from 1977 through 2017. Note that the climate boundary was not activated in the numerical model until the end of wall construction.

Figure 8. Annual Cumulative Precipitation, *P*, And Potential Evapotranspiration, ET_o

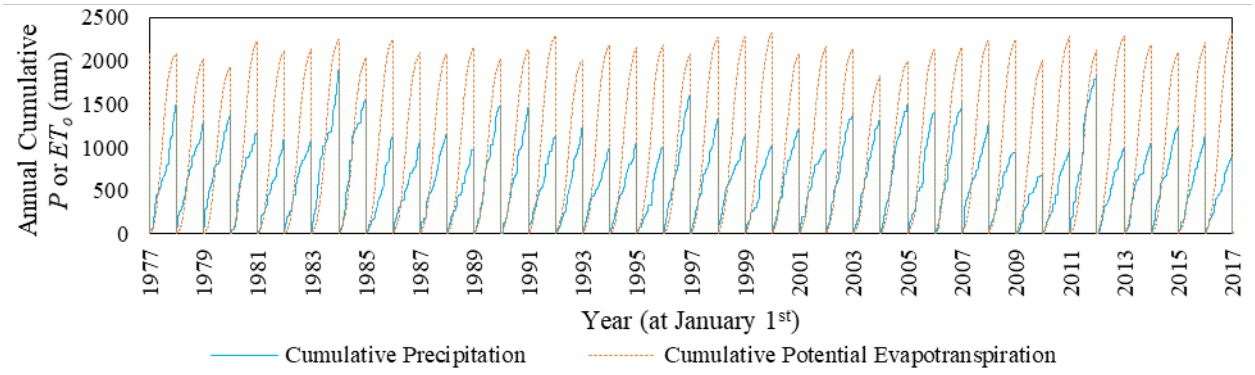

5.3 Initial Conditions

To simulate wall construction in this study, fill layers were activated in the model incrementally. Each layer was loaded by a surcharge equivalent to the weight of the subsequent layer in a similar approach to the surface-pressure procedure (Lefebvre and Duncan 1971; Palmerton and Lefebvre 1972). To allow for transient hydraulic changes during construction, the surcharge was applied on each layer for a period equivalent to one half of the time required for the construction of one layer. After the surcharge removal and the activation of the subsequent layer, an additional period equivalent to the second half of the time required for the construction of one layer was allowed (Morsy et al. 2023; Morsy and Helm 2024). During the second half, a surcharge of 8 kPa was applied on the reinforced fill layers to account for the effect of compaction (Bathurst et al. 2008). A compaction surcharge was applied at 1 m away from the back of the facing (Taylor et al. 2023), which is typically compacted with lighter, smaller compactors rather than heavy compaction machinery. This has been common practice since the 1970s and was adopted in the specifications of the Westchester County case study walls.

5.4 Reinforcement Modeling

Reinforcements were modeled using the strip element model in FLAC, which is specifically designed to simulate the behavior of thin, flat reinforcing strips placed in layers within a fill structure, including reinforced soil walls (Itasca 2019). The strip elements can sustain tension or compression but cannot sustain flexure. Strip element models have been used in metallically reinforced MSE wall modeling in the literature (e.g., Abdelouhab et al. 2010; Yu et al. 2015; Lajvardi and Dias 2021). Strip elements also allow assigning zero-thickness interface properties to model the soil-reinforcement interface behavior. Interface shear behavior is defined by a nonlinear shear failure envelope that varies as a function of normal stress. Reinforcements were discretized into segments of approximately 0.25 m and were pinned to the facing to simulate the behavior of typical facing connections.

According to the specifications from the 1970s (see Table 1), reinforcements used in the construction of MSE walls were smooth strips manufactured as per ASTM A446 Grade C. The yield strength and Young's modulus of the reinforcements were assumed to be 2.9×10^5 kPa and 2.1×10^8 kPa respectively. The length of the reinforcement strips was taken as 70% of the wall height and their width was taken as 60 mm. Reinforcement steel base thickness was taken as 3 mm with a zinc coating thickness of 65 μm as per ASTM A525 class G210. The soil-reinforcement interface was modeled with a shear stiffness of 1×10^6 kN/m/m (Itasca 2019), adhesion of 1×10^4 kN/m (Itasca 2019), and an apparent friction coefficient, F^*, of 0.4 (AASHTO 2020).

It is notable that the corrosion rate in the field is in constant variation (Cai et al. 2018), as the conditions that contribute to corrosion vary continuously, which may result in time lags between the state of the parameters and the corrosion rate (Daneshian et al. 2023). Accordingly, a detailed understanding of the effect of weather on corrosion based on the available discrete data is not possible unless the variation of the conditions contributing to corrosion can be predicted at the location of the corroding reinforcement. Accordingly, reinforcements were modeled to corrode variably with time and in response to the moisture variation within the reinforced fill. In this study, an emphasis has been placed on soil moisture content and soil resistivity in determining the corrosion rate and its variation with time.

The study attempted to develop an improved model to predict corrosion rate under specific conditions, independent of time, to realistically reflect the expected corrosion of steel reinforcements considering wall fill type, moisture, and resistivity. The relationship between reinforcement corrosion rate and soil resistivity can be expressed using a power function as follows:

$$CR = K.\left(\frac{\rho}{\rho_w}\right)^r$$

where K and r are constants that depend on soil type and account for other parameters that contribute to corrosion (e.g., chloride content, sulfate content, pH value, organic content). The value of the resistivity exponent, r, ranges from -0.84 to -0.34 (Fishman and Withiam 2011; Fishman et al. 2021). In the absence of long-term monitoring data of corrosion and the corresponding parameters contributing to corrosion, a preliminary corrosion rate model was suggested in this study to present the deterioration modeling framework. An improved, comprehensive corrosion rate model is currently under development by the authors to account for the key parameters contributing to corrosion as more data is compiled through controlled experimentation and long-term field monitoring.

5.5 Soil Modeling

The reinforced, retained, and embedment soils were modeled using a linearly-elastic-perfectly-plastic Mohr-Coulomb model. This model has been used extensively in the literature to model

soils in reinforced soil walls (Zevgolis and Bourdeau 2007; Abdelouhab et al. 2010; Aubeny et al. 2014; Kibria et al. 2014; Damians et al. 2013, 2021; Yu et al. 2015). Mean effective normal stresses, σ'_m, were modeled based on Bishop's generalized effective stress (Bishop 1959), as $\sigma'_m = \sigma_m - u_a + \chi(u_a - u_w)$, where σ_m is the mean total normal stress, u_a is the pore-air pressure, u_w is the pore-water pressure, and χ is Bishop's effective stress parameter, which can be approximated to the degree of water saturation, S_w. For simplicity, the same constitutive model was adopted for all soils involved in the modeled hypothetical wall. The friction angle, ϕ', was taken as 37 degrees, the dilatancy angle, ψ', was taken as $\phi' - 30$ as suggested by Bolton (1986) for sands, and the cohesion, c', was taken as 1 kPa. Young's modulus, E, was taken as 6×10^4 kPa and Poisson's ratio, υ, was taken as 0.3. The dry unit weight, γ_d, was taken as 16 kN/m^3, and the porosity, n, was taken as 0.4.

5.6 Facing Modeling

The facing was assumed to be 1.5 m × 1.5 m segmental concrete panels, which was modeled using a grided volume with assigned concrete properties. The thickness of the facing was taken as 0.15 m. A linear-elastic model was used to simulate the mechanical behavior of the facing. A zero-thickness interface model was used to simulate the interface behavior at the contact surface between the reinforced fill and the back of the facing. The interface was modeled using interface shear and normal stiffnesses of 2×10^6 kPa/m and 2×10^6 kPa/m respectively (Itasca 2019) and an interface friction angle of 25 degrees (0.67 of the reinforced fill friction angle). Young's modulus, E, was taken as 2×10^7 kPa and Poisson's ratio, υ, was taken as 0.15. The unit weight, γ, was taken as 20 kN/m^3, and the porosity, n, was taken as 0.1.

5.7 Pore Fluid Modeling

The pore fluids (i.e., water and air) were treated as two immiscible fluids that can only displace each other during transient flow calculations with no mass transfer between them (Itasca 2019). To compensate for this assumption, the water bulk modulus, K_w, was set to 1×10^5 kPa (Itasca 2019), which considers the effect of the dissolved air in the water phase on its bulk modulus. The air bulk modulus, K_g, was set to 5 kPa. Soil particles forming the soil skeleton were assumed to be incompressible.

The soil-water retention curves were represented using the van Genuchten (1980) fitting model as $\psi_m = u_a - u_w = \psi_{m,o}\left({S_e}^{-1/a_{vg}} - 1\right)^{1-a_{vg}}$, where ψ_m is the matric suction (i.e., the difference between the pore-air and pore-water pressures); $\psi_{m,o}$ is a fitting parameter that can be related to the matric suction at air entry, which was taken as 50 and 10 kPa for the fills and the concrete facing of the modeled exemplar wall respectively; a_{vg} is a fitting parameter, which was taken as 0.25; and S_e is the effective saturation, which can be expressed as $S_e = \frac{S_w - S_{w,r}}{1 - S_{w,r}}$, where S_w is the degree of water saturation and $S_{w,r}$ is the residual degree of water saturation, which was taken as 0.0 for the fills and 0.65 for the concrete facing. Since the pore fluids are treated as two immiscible

fluids that can only displace each other within the void volume, the degree of gas saturation, S_g, can be expressed in terms of the degree of water saturation as $S_g = 1 - S_w$.

The hydraulic conductivity functions were correlated to the soil-water retention curves using the van Genuchten-Mualem model (Mualem 1976; van Genuchten 1980) as $k_w = \kappa_{r,w}\ k_{w,sat}$, where k_w is the hydraulic conductivity, $k_{w,sat}$ is k_w at $S_w = 1$, and $\kappa_{r,w}$ is the relative hydraulic conductivity, which can be expressed as $\kappa_{r,w} = {S_e}^{0.5}\left[1 - \left(1 - {S_e}^{1/a_{vg}}\right)^{a_{vg}}\right]^2$. The value of $k_{w,sat}$ was taken as a low value within the range of $k_{w,sat}$ for typical silty sands. Lower $k_{w,sat}$ delays the drainage of water infiltrating into the reinforced fills, allowing them to maintain elevated moisture levels and consequently exacerbate reinforcement corrosion. Given that the specifications of reinforced fills permitted fines content up to 25% during the construction of early-generation reinforced soil walls (fines content are limited to 15% in current practice), a worst-case scenario approach was adopted in this study. Values of $k_{w,sat}$ of 1×10^{-8} and 1×10^{-6} m/s were used in the trials conducted in this study. A value of 1×10^{-12} m/s was assigned for the $k_{w,sat}$ of the concrete facing.

The air conductivity functions were correlated to those of the hydraulic conductivity (Parker et al. 1987) as $k_g = \kappa_{r,g}\ k_{g,sat}$, where k_g is the gas conductivity, and $k_{g,sat}$ is k_g at $S_w = 1$, which was correlated to the saturated hydraulic conductivity and water-to-air dynamic viscosity ratio, μ_r (μ_r = 55), as $k_{g,sat} = \gamma_g\ \mu_r\ k_{w,sat}$, and $\kappa_{r,g}$ is the relative gas conductivity, which can be expressed as $\kappa_{r,g} = (1 - S_e)^{0.5}\left(1 - {S_e}^{1/a_{vg}}\right)^{2a_{vg}}$.

5.8 Pilot Results

This section presents the type of output data that can be produced by the developed numerical model and explains how this data can be used to develop performance models for reinforced soil walls (discussed in the next section). Two datasets are presented herein that show varied levels of moisture fluctuations within the reinforced fill: (a) saturation fluctuation between 75% and 100% (wet case); and (b) saturation fluctuation between 25% and 50% (dry case). For each dataset, two scenarios were assumed for the corrosion onset of the base steel of the reinforcements: (i) corrosion immediately after construction and exposure to moisture; and (ii) corrosion after the depletion of the zinc coating (11 years in this case). Figure 9a shows an example for the weather-driven moisture variation of the reinforced fill (expressed by the soil degree of saturation) with time in the vicinity of a given reinforcement layer. Figure 9b shows an example for the variation of reinforced fill resistivity with time in response to the moisture variation, where resistivity decreases with increasing moisture.

Figure 9. Example of the Variation of (A) Reinforced Fill Moisture with Time; And (B) Reinforced Fill Resistivity with Time.

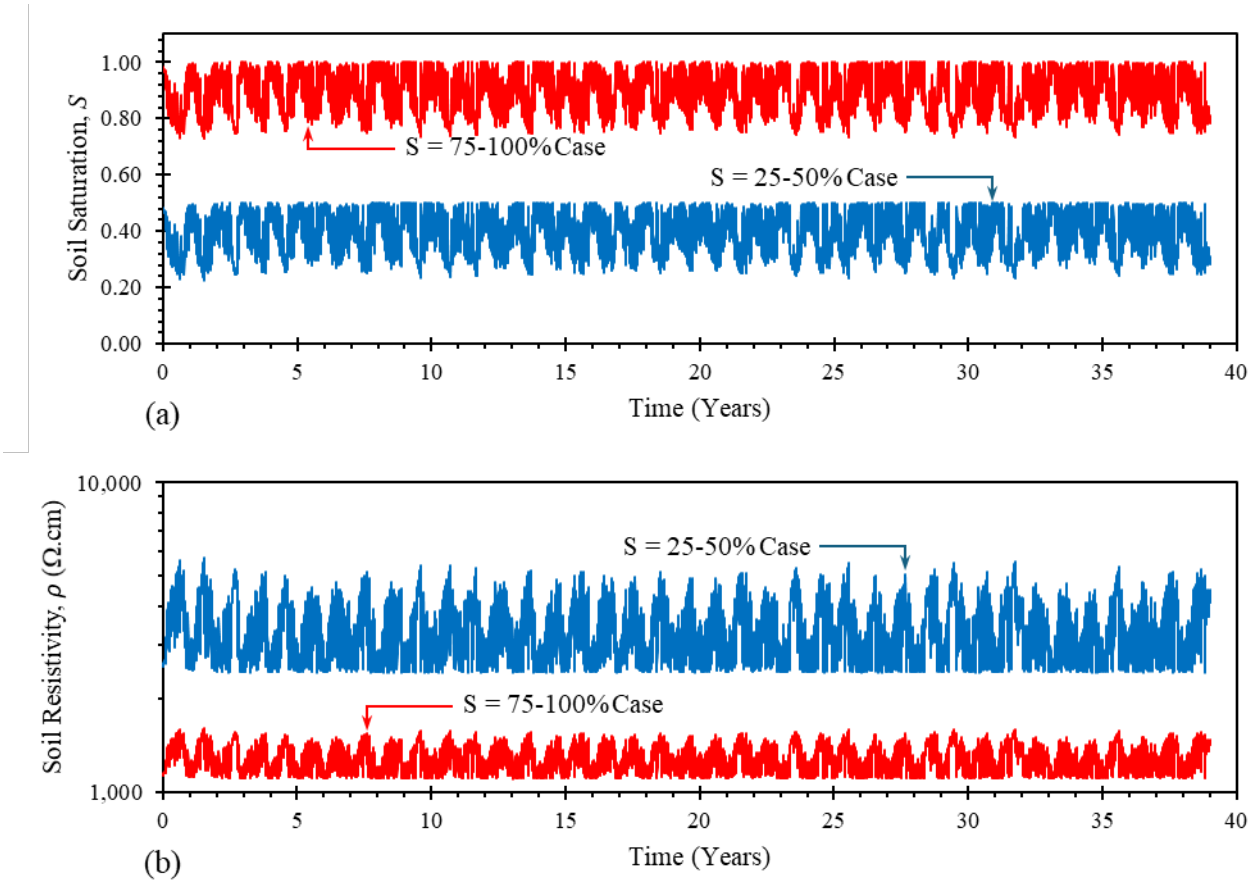

To correlate the corrosion rate with the reinforced fill and its resistivity using the framework presented earlier, end-life corrosion data from the Westchester County wall case studies was used to back-calculate the value of the corrosion model coefficient, *K*. The value of the resistivity exponent, *r*, was taken in this study as –0.7. As part of the investigation that Westchester County case study walls underwent, reinforcements were exhumed from the failed sections to evaluate the extent of corrosion they had experienced. Additionally, samples from the reinforced fill were collected to evaluate its electrochemical properties at various locations and elevations. Figure 10 shows the corrosion of the exhumed reinforcements across the reinforced fill zone. It is notable that the corrosion was found to be the highest near the wall facing. Accordingly, data within the 1 m behind the wall facing were used to perform a worst-case scenario back-analysis. The back-analysis was performed considering the mean (μ), mean + 1 standard deviation (μ + σ), and mean – 1 standard deviation (μ – σ) of the corrosion measurements.

Figure 10. End-Life Reinforcement Thickness Loss Measured in NY MSE Wall Case Studies: (A) Wall No. 1; (B) Wall No. 2

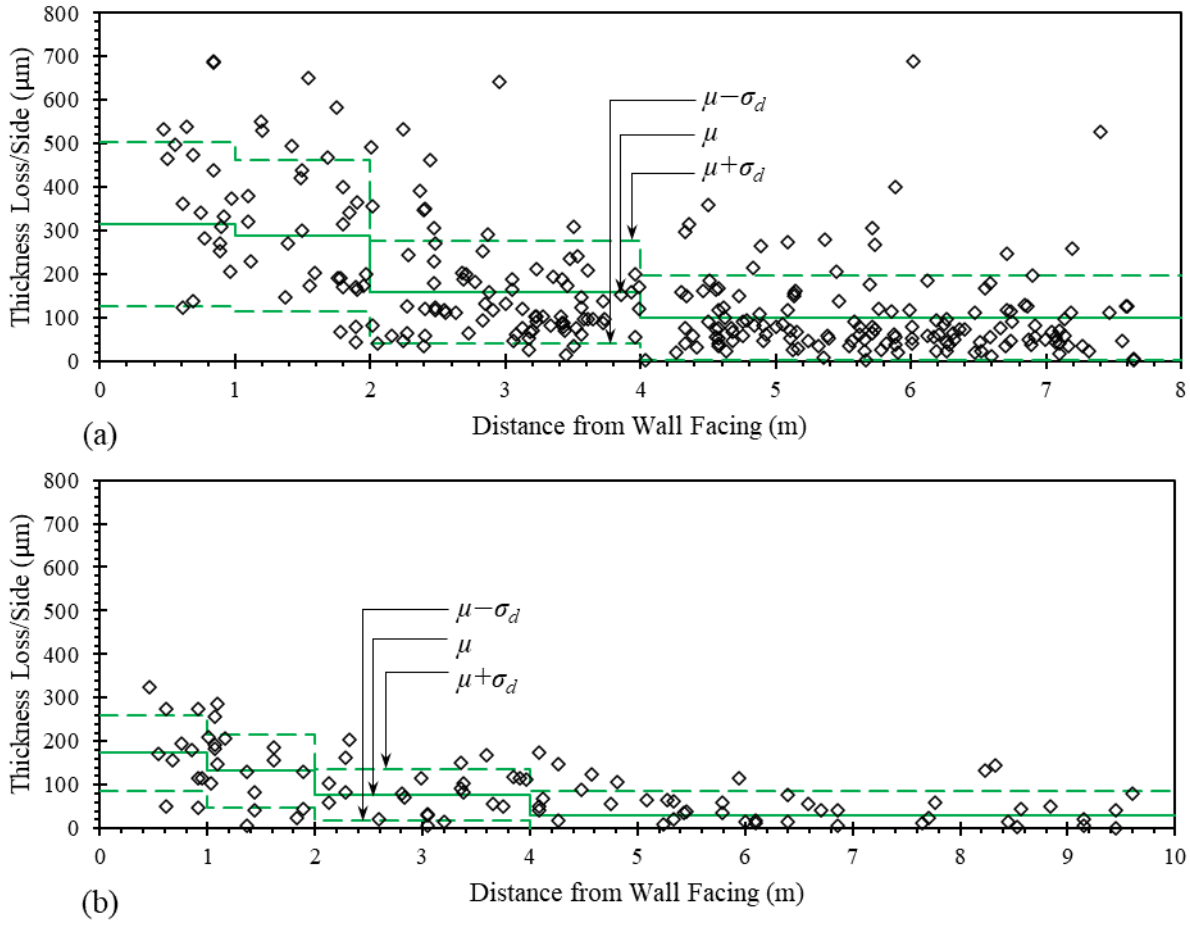

Data in the figure are processed from original weight loss measurements provided by NYSDOT.

Figure 11 presents the variation of reinforcement corrosion rate with time in response to the fill resistivity variation, where corrosion rate increases with decreasing resistivity. Figure 12 shows an example of cumulative thickness loss (per reinforcement side) using the *K* values back-calculated considering μ, μ + σ, and μ − σ of the corrosion data for both datasets, S = 75–100% (wet) and S = 25–50% (dry). The AASHTO corrosion model is also plotted for comparison purposes. As shown in Figure 12, despite the fluctuation of the corrosion rate, the rate of increase in cumulative thickness loss with time is fairly constant (or can be practically approximated as a constant rate). This indicates that 25% fluctuation in the degree of saturation may not necessitate further improvement in predicting the degree of saturation over time and for the entire service life of the wall. Alternatively, average seasonal climate (one-year average climate records) at the wall geographic location may produce the variation in fill moisture necessary to predict the amount of corrosion that reinforcements can experience in one service year.

Figure 11. Example of the Variation of Corrosion Rate with Time

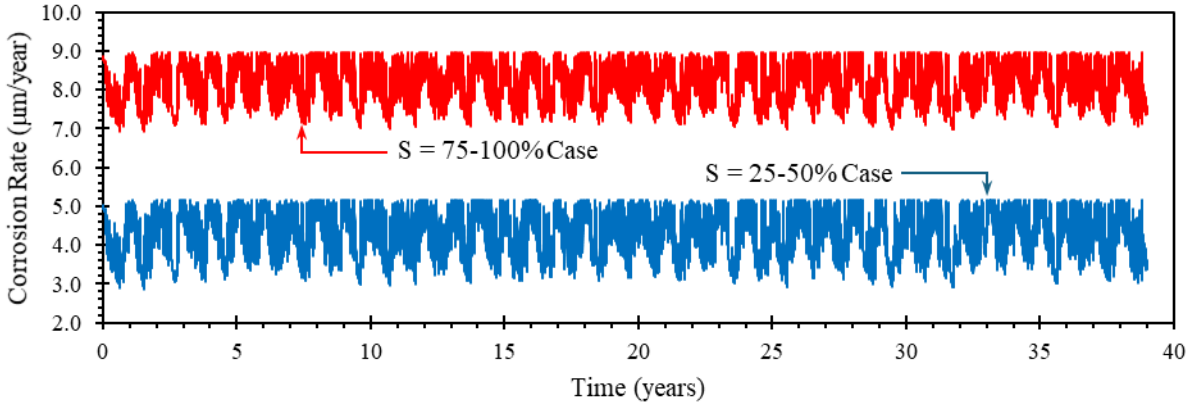

Figure 12. Examples of Cumulative Thickness Loss with Time: (A) Corrosion Immediately after Construction and Exposure to Moisture; and (B) Corrosion after the Depletion of the Zinc Coating (11 Years in This Case)

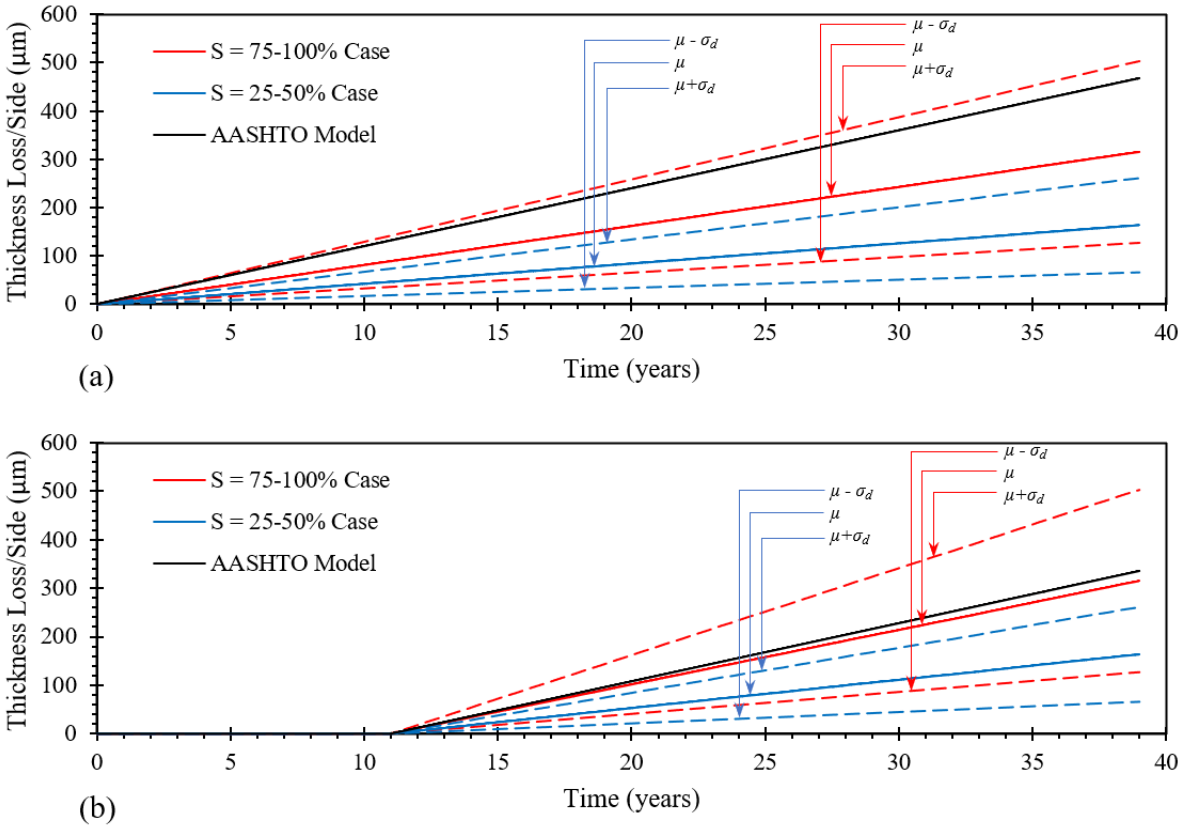

6. Performance Modeling for Asset Management

AASHTO (1996) defines asset management as "a systematic process of maintaining, upgrading, and operating physical assets cost-effectively. It combines engineering principles with sound business practices and economic theory, and it provides tools to facilitate a more organized, logical approach to decision-making." Accordingly, asset management provides a framework for both short-term and long-term planning and informed decision-making regarding assets. Asset management incorporates the economic assessment of trade-offs between alternative investment options at both the project level and the network or system level, which can assist infrastructure stakeholders to make informative, cost-effective decisions regarding their assets.

6.1 Risk-Based Asset Management

Risk is the positive or negative effect of uncertainty or variability on agency objectives (AASHTO 2016). Risk can be evaluated based on asset vulnerability and its failure consequences (FHWA 2012), as shown in Figure 13. Risk allows uncertainty to be incorporated into the asset management process by identifying sources of risk, evaluating them, and integrating mitigation actions and strategies into the routine business functions of the agency. This can be achieved by addressing (1) the likelihood of a given asset failing to perform its intended function, (2) the consequence associated with the failure of a given asset, and (3) the age at which a given asset is likely to fail (Govindasamy et al. 2018). This study aimed to harness numerical modeling capabilities to contribute to addressing the first and third items.

Figure 13. Components of Risk

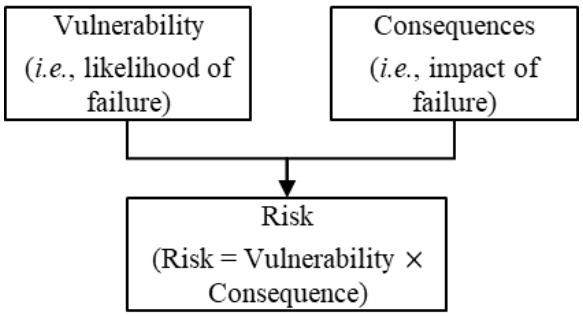

Vulnerability is an indicator of the failure likelihood of a wall. It can be quantified by determining the safety margins associated with the various internal failure modes of a reinforced soil wall (e.g., reinforcement rupture, reinforcement pullout). Since the focus of this study is about asset deterioration due to metallic reinforcement corrosion as the main deterioration mechanism of MSE walls, reinforcement rupture was used to evaluate the reduction in the safety margin as a wall deteriorates with time. This evaluation can lead to performance prediction of a given asset as it ages with time, which can be extrapolated using numerical model predictions from several model simulations considering a range of wall parameters.

6.2 Performance Modeling

The ultimate objective of this research is to predict the time to failure of progressively deteriorating walls. The asset-scale model can be used to run numerical simulations to generate data necessary to develop performance models based on a performance-requirement failure framework, as shown in Figure 14. In this framework, and for a given failure mode, the performance can be represented by a performance indicator (e.g., reinforcement tensile capacity) and the requirement can be represented by a predefined minimum required performance below which failure is considered to have occurred. This framework can consider the uncertainty in evaluating the performance using a probabilistic approach rather than a deterministic approach.

Figure 14. Performance-Requirement Failure Model

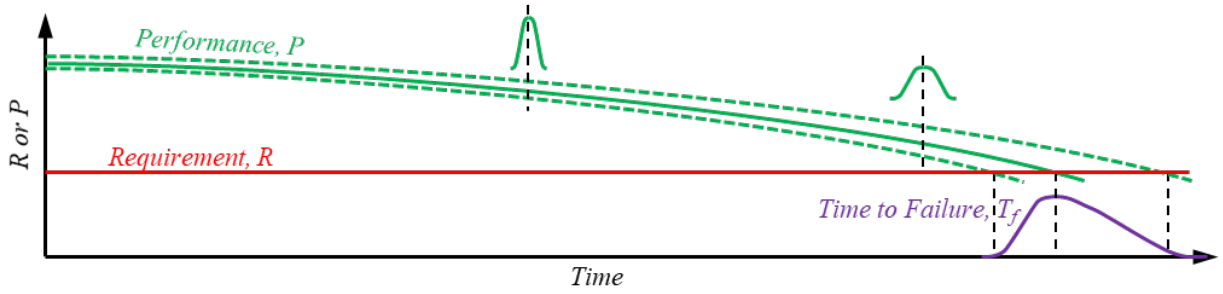

This study used the reinforcement tensile capacity as a performance indicator and used a predefined factor of safety against reinforcement rupture as a requirement to develop a performance model framework for reinforced soil walls using the data generated by the numerical model developed in this study. The performance model shall facilitate the interpretation of the computer model outputs in engineering practice. Figure 15a presents an example for predicted tensile force time history obtained from the asset-scale numerical model for a given reinforcement at the facing. The figure also shows the tensile capacity of the reinforcement as it reduces with time due to cumulative corrosion. Figure 15b shows an example for the variation of the factor of safety against reinforcement rupture with time. According to this example, the factor of safety against reinforcement rupture of the reinforcement analyzed in this illustrative example is expected to drop to 1.0 (i.e., onset of failure) at an age of approximately 33.5 years.

It is notable that other long-term performance indicators can also be predicted using the asset-scale numerical model, such as time-dependent settlement, lateral displacements, and other metrics that can be practically obtained from the field for existing aged walls. Such metrics are deemed more pragmatic for asset management purposes for aged walls with no prior monitoring data. Figure 16 shows an example for the cumulative lateral displacement of a wall with time and the range of the typical acceptable lateral displacement as per Taylor et al. (2023), which is 2 to 4 inches (50 to 100 mm). A lateral displacement limit of 1% of wall height is also shown in Figure 16, which is often used for reinforced soil bridge abutments.

Figure 15. Example of the Performance-Requirement Failure Model: (A) Tensile Force vs. Tensile Capacity Variation with Time; And (B) Factor of Safety Against Reinforcement Rupture Variation with Time

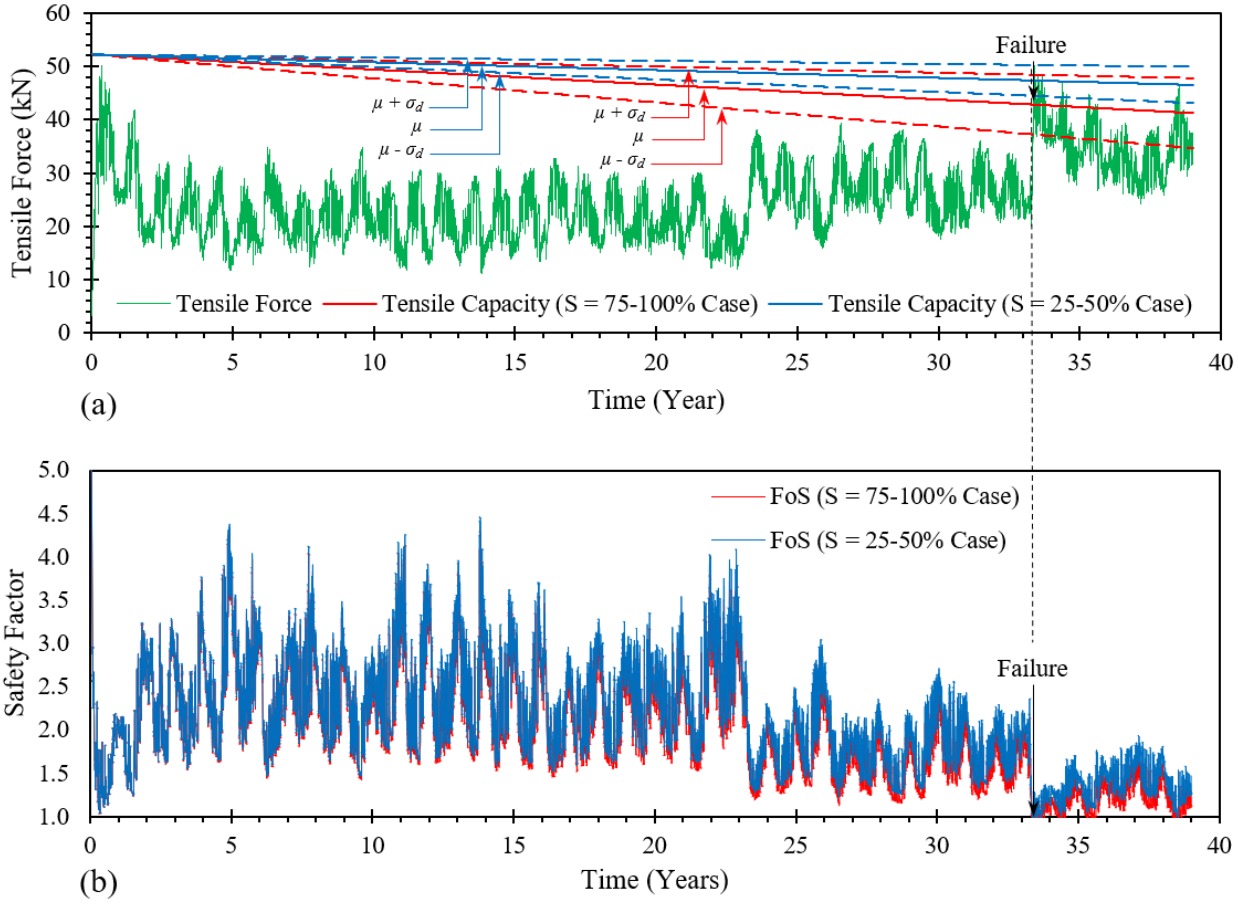

Figure 16. Example of the Performance-Requirement Failure Model Using Lateral Displacement as a Performance Indicator

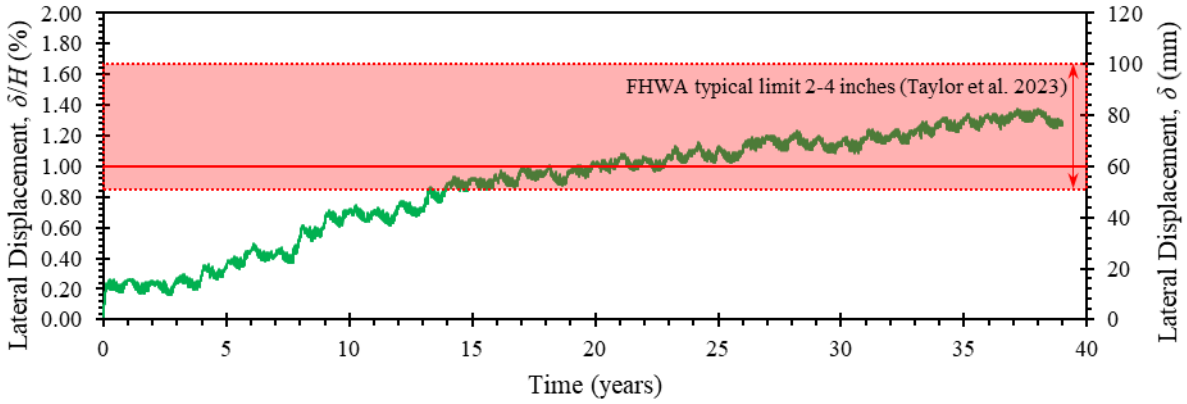

7. Summary and Recommendations

Reinforced soil retaining walls, like all infrastructure assets, have lifespans beyond which they cease to perform their intended functions. Failure of reinforced soil walls can result in severe and costly consequences, including disruption to the mobility of users, goods, and services. Unexpected failures can impose significant burdens on the limited resources of infrastructure stakeholders. The service life of a reinforced soil wall is governed by several deterioration mechanisms that may have different onsets and collectively can result in functional failures over time. Deterioration can generally be difficult to quantitatively predict, but it is undoubtedly impossible to predict by visual inspections. Therefore, the service life of reinforced soil walls is often uncertain, which results in excessively expensive risk mitigation measures and inefficient allocation of limited resources. Additionally, the evolution in the design and construction specifications of reinforced soil walls pertaining to the characteristics of reinforced fill, reinforcement, and galvanization adds to the uncertainty regarding long-term asset performance. Some specifications adopted in the past are deemed unacceptable in accordance with current specifications (Govindasamy et al. 2018), indicating inadequate conditions of a considerable number of existing early-generation reinforced soil wall assets.

This study used advanced numerical modeling approaches to offer valuable insights into the behavior and long-term performance of reinforced soil walls for asset management purposes. An asset-scale hydromechanical numerical model was developed for a reinforced soil wall constructed with metallic reinforcement and subject to weather conditions. A material-scale reinforcement model that accounts for moisture-driven corrosion was incorporated into the asset-scale numerical model. This allowed reinforcements to corrode with time at continuously varying rates in response to the varying moisture levels within the reinforced fill at the respective location of each reinforcement. Such a numerical model can predict the long-term performance indicators, such as time-dependent settlement, reinforcement strains, lateral displacements, and other stability metrics, which are necessary for vulnerability assessment of reinforced soil walls.

An asset-scale performance model based on a performance-requirement failure framework was developed using the outputs of the asset-scale numerical model. In this study, and by way of example, reinforcement tensile strength was used as a performance indicator. As reinforcements progressively corrode and their cross-sections reduce, their tensile strength diminishes to a point where they can no longer sustain the tensile stresses exerted on them by the reinforced fill. Other performance indicators suggested by this study include lateral displacement, which may be a practical indicator for existing aged walls that can only be monitored for external deformation. These performance models can serve as decision support tools by providing physics-based quantitative data for informed decisions about maintenance, repair, or replacement strategies, and optimizing the allocation of resources.

It is notable that the numerical model presented here requires validation using well-documented case studies with long-term performance monitoring data before it can be used to generate the data necessary to develop performance models for reinforced soil walls of varied characteristics.

7.1 Research Gaps

Data generated in past studies to evaluate reinforcement corrosion in reinforced soil walls is limited to fills that classify as sands and gravels with limited fines content—typically less than 15%, which is in line with current construction practices of reinforced walls (Fishman et al. 2021). However, earlier reinforced soil wall generations may have been constructed with fines content larger than 15% and up to 25% as allowed by the specifications available at the time of their construction (see Table 2). Also, according to Fishman et al. (2021), in some states, fills with fines content larger than 15% have been common in reinforced soil wall construction. Accordingly, more data is needed to facilitate the characterization of reinforcement corrosion in fills with a wide range of fines content (i.e., varied percent by weight passing sieve No. 200), plasticity (i.e., varied plasticity index), and minerology (i.e., varied cation exchange capacity). Additionally, data generated in past studies to evaluate reinforcement corrosion in reinforced soil walls and its variation with time (as fill conditions continuously vary) is very scarce (NASEM 2023). Long-term longitudinal field monitoring data of soil moisture, resistivity, salt concentration, pH value, and corrosion rate are needed to validate the existing field and experimental databases and corrosion models. Finally, extensive experimental programs that recreate instantaneous field conditions may be needed to evaluate time-independent corrosion rates that correspond to varied combinations of the key fill parameters contributing to corrosion. Data from such controlled experiments can be very efficient in improving corrosion models that may otherwise require very long, time-expensive field monitoring data from multiple walls and sites.

7.2 Ongoing Research

The study presented in this report is part of an ongoing effort at California State University, Long Beach to develop physics-based deterioration models for reinforced soil walls constructed using metallic reinforcements. This includes (1) improving the material-scale reinforcement model to consider the key parameters contributing to corrosion, (2) calibrating the material-scale reinforcement model using data from controlled experimentation and continuous field monitoring, (3) validating the mechanical and hydraulic behaviors of the numerical model using well-documented case studies with long-term field monitoring data, and (4) performing numerical simulations with varied wall and climate characteristics.

7.3 Recommendations

This study presents an asset-scale numerical model for an exemplary reinforced soil wall representative of the early-generation reinforced soil walls constructed in the 1970s. The numerical model considers soil hydromechanical behavior, which allows prediction of fill moisture

fluctuations with time. The model also incorporates a reinforcement-scale deterioration model that allows reinforcements to deteriorate with time during the numerical simulation. The model was used to investigate corrosion trends with time for wall cases with wet fills (degree of saturation varying between 75% and 100%) and dry fills (degree of saturation varying between 25% and 50%), based on the water retentivity and hydraulic conductivity of the reinforced fill. The preliminary results of this study indicate that despite the fluctuation of reinforcement corrosion rates associated with the fluctuations of fill moisture, the rate of increase in cumulative thickness loss (i.e., cumulative corrosion) with time is fairly constant—that is, the relationship between cumulative corrosion and time is approximately linear, which is consistent with the corrosion models adopted in current practice. It is notable that the material-scale reinforcement model used in this study conservatively does not consider the formation of rust scales on corroded reinforcements, which tend to slow down the corrosion process over time. In conclusion, this observation supports current practices that use linear models with time to predict cumulative corrosion.

The results of this study indicate that fill moisture may have a considerable effect on the rate of corrosion. Unlike newer wall generations constructed with strict specifications that limit fill corrosivity, early-generation reinforced soil walls may maintain high moisture levels for prolonged periods that can significantly increase corrosion rates. Accordingly, it is recommended that fill moisture monitoring be added to early-generation reinforced soil walls that could have been constructed with highly corrosive and poorly drainable fills as part of their asset management. Such monitoring data can be useful to make proper predictions based on field conditions.

The results of this study also indicate that 25% fluctuation in fill moisture has little to no effect on the cumulative corrosion and that the average fill moisture (with no fluctuation) can be used to predict long-term cumulative corrosion. Accordingly, it is recommended that average seasonal climate records (one-year average climate records) be used at a given geographic location to produce the one-year variation in fill moisture necessary to predict the amount of corrosion that reinforcements can experience in one service year, which can be multiplied by the number of service years to predict long-term cumulative corrosion.

Bibliography

AASHTO (1990). *In-situ soil improvement techniques*. AASTHO-AGV ARBTA Joint Committee, Subcommittee on New Highway Materials, Task Force 27 Report, American Association of State Highway and Transportation Officials (AASHTO).

AASHTO (1991). *Standard specifications for highway bridges*. 1991 Interim Revisions, American Association of State Highway and Transportation Officials (AASHTO).

AASHTO (1996). Asset management: Advancing the state of the art into the 21st century through public-private dialogue, *Proceedings of the Executive Seminar on Asset Management*, Washington, DC.

AASHTO (1999). *Asset management primer*. American Association of State Highway and Transportation Officials (AASHTO).

AASHTO (2009). *AASHTO transportation glossary*. 4th Edition. American Association of State Highway and Transportation Officials (AASHTO).

AASHTO (2016). *AASHTO Guide for enterprise risk management*. American Association of State Highway and Transportation Officials (AASHTO).

AASHTO T-99 (2017). *Moisture-density relations of soils and soil-aggregate mixtures using 5.5-lb (2.5-kg) rammer and 12-in.(305-mm) drop*. American Association of State Highway and Transportation Officials (AASHTO).

AASHTO T-180 (2017). *Moisture-density relations of soils and soil-aggregate mixtures using 10-lb (4.54-kg) rammer and 18-in.(457-mm) drop*. American Association of State Highway and Transportation Officials (AASHTO).

AASHTO T-288 (2023). *Standard method of test for determining minimum laboratory soil resistivity* American Association of State Highway and Transportation Officials (AASHTO).

AASHTO (2017). *AASHTO LRFD bridge design specifications*. American Association of State Highway and Transportation Officials (AASHTO).

Abdelouhab, A., Dias, D., & Freitag, N. (2011). Numerical analysis of the behaviour of mechanically stabilized earth walls reinforced with different types of strips. *Geotextiles and Geomembranes*, *29*(2), 116–129. https://doi.org/10.1016/j.geotexmem.2010.10.011

Adams, M. T., & Nicks, J. E. (2017). Development of a risk assessment for MSE wall projects. In *Geotechnical Frontiers 2017* (pp. 94–101).

Allen, R. G., Pereira, L. S., Raes, D., & Smith, M. (1998). Crop evapotranspiration-Guidelines for computing crop water requirements-FAO Irrigation and drainage paper 56. *Fao, Rome*, *300*(9), D05109.

Anderson, S. A., Alzamora, D., & DeMarco, M. J. (2009). Asset management systems for retaining walls. In *Geo-Velopment: The role of geological and geotechnical engineering in new and redevelopment projects* (pp. 162–177).

Archie, G. E. (1942). The electrical resistivity log as an aid in determining some reservoir characteristics. *Transactions of the AIME*, *146*(1), 54–62. https://doi.org/10.2118/942054-G

Arif, F., & Bayraktar, M. E. (2012). Theoretical framework for transportation infrastructure asset management based on review of best practices. In *Construction Research Congress 2012: Construction Challenges in a Flat World* (pp. 2349–2358).

Athanasopoulos-Zekkos, A., Lynch, J., Zekkos, D., Grizi, A., Admassu, K., Benhamida, B., ... & Mikolajczyk, M. (2020). Asset management for retaining walls (No. SPR-1676). Michigan. Dept. of Transportation. Research Administration.

Aubeny, C. P., Biscontin, G., Huang, J., Dantal, V. S., Sadat, R., & Bin-Shafique, S. (2014). *Design parameters and methodology for mechanically stabilized earth (MSE) walls* (No. FHWA/TX-14/0-6716-1). Texas A&M Transportation Institute.

Bathurst, R. J., Walters, D. L., Hatami, K., Saunders, D. D., Vlachopoulos, N., Burgess, P. G., & Allen, T. M. (2002, September). Performance testing and numerical modelling of reinforced soil retaining walls. In *Proceedings of the 7th International Conference on Geosynthetics, Nice, France* (pp. 22–27).

Bathurst, R. J., Huang, B., & Hatami, K. (2008). Numerical modelling of geosynthetic reinforced retaining walls. *International Association for Computer Methods and Advances in Geomechanics (IACMAG), Goa, India*, 1–6.

Bathurst, R. J., Huang, B., & Allen, T. M. (2011). Analysis of installation damage tests for LRFD calibration of reinforced soil structures. *Geotextiles and Geomembranes*, *29*(3), 323–334. https://doi.org/10.1016/j.geotexmem.2010.10.003

Berg, R. R., Christopher, B. R., & Samtani, N. C. (2009a). *Design and construction of mechanically stabilized earth walls and reinforced soil slopes*. *Volume I*. Report No. FHWA-NHI-10-024, US Department of Transportation, Federal Highway Administration, National Highway Institute.

Berg, R. R., Christopher, B. R., & Samtani, N. C. (2009b). *Design and construction of mechanically stabilized earth walls and reinforced soil slopes. Volume II*. Report No. FHWA-NHI-10-025, US Department of Transportation, Federal Highway Administration, National Highway Institute.

Bernhardt, K. L., Loehr, J. E., & Huaco, D. (2003). Asset management framework for geotechnical infrastructure. *Journal of Infrastructure Systems*, *9*(3), 107–116. https://doi.org/10.1061/(ASCE)1076-0342(2003)9:3(107)

Bishop, A. W. (1959). The principal of effective stress. *Teknisk ukeblad*, *106*(39), 859–863.

Biondini, F., & Frangopol, D. M. (2016). Life-cycle performance of deteriorating structural systems under uncertainty: Review. *Journal of Structural Engineering*, *142*(9), F4016001. https://doi.org/10.1061/(ASCE)ST.1943-541X.0001544

Bolton, M. D. (1986). The strength and dilatancy of sands. *Geotechnique*, *36*(1), 65–78. https://doi.org/10.1680/geot.1986.36.1.65

Bourgeois, E., Corfdir, A., & Chau, T. L. (2013). Analysis of long-term deformations of MSE walls based on various corrosion scenarios. *Soils and foundations*, *53*(2), 259–271. https://doi.org/10.1016/j.sandf.2013.02.006

Bowman, E. T., & Soga, K. (2003). Creep, ageing and microstructural change in dense granular materials. *Soils and Foundations*, *43*(4), 107–117. https://doi.org/10.3208/sandf.43.4_107

Breckwoldt, C. V., Parsons, R., & Han, J. (2019). *Investigation of variations in corrosion potential in Mechanically Stabilized Earth backfill due to migration of fines*. Report No. K-TRAN: KU-18-5, Kansas Department of Transportation.

Bronson, A., Castillo, C., Hinojos, J., Nazarian, S., & Borrok, D. (2020). Relating corrosion of Mechanically Stabilized Earth reinforcements with fluid conductivity of backfill soils. *Journal of Materials in Civil Engineering*, *32*(11), 04020346. https://doi.org/10.1061/(ASCE)MT.1943-5533.0003431

Brutus, O., & Tauber, G. (2009). *Guide to asset management of earth retaining structures* (pp. 1–120). Washington, DC, USA: US Department of Transportation, Federal Highway Administration, Office of Asset Management.

Butler, C. J., Gabr, M. A., Rasdorf, W., Findley, D. J., Chang, J. C., & Hammit, B. E. (2016). Retaining wall field condition inspection, rating analysis, and condition assessment. *Journal of Performance of Constructed Facilities*, *30*(3), 04015039. https://doi.org/10.1061/(ASCE)CF.1943-5509.0000785

Cai, Y., Zhao, Y., Ma, X., Zhou, K., & Chen, Y. (2018). Influence of environmental factors on atmospheric corrosion in dynamic environment. *Corrosion Science*, *137*, 163–175. https://doi.org/10.1016/j.corsci.2018.03.042

Chambers, J. E., Gunn, D. A., Wilkinson, P. B., Meldrum, P. I., Haslam, E., Holyoake, S., Kirkham, M., Kuras, O., Merritt, A., & Wragg, J. (2014). 4D electrical resistivity tomography monitoring of soil moisture dynamics in an operational railway embankment. *Near Surface Geophysics*, *12*(1), 61–72. https://doi.org/10.3997/1873-0604.2013002

Christopher, B. R., Gill, S. A., Giroud, J. P., Juran, I., Mitchell, J. K., Schlosser, F., & Dunnicliff, J. (1989a). *Design and construction guidelines for reinforced soil structures–volume I*. Report FHW ARD-89-043, Federal Highway Administration (FHWA).

Christopher, B.R., Gill, S.A., Giroud, J.-P., Juran, I., Mitchell, J.K., Schlosser, F., & Duncliff, J. (1989b). *Design and construction guidelines reinforced soil structures–volume II*. Report No. FHWA-89-043, Federal Highway Administration (FHWA).

Costerton, J. W., Cheng, K. J., Geesey, G. G., Ladd, T. I., Nickel, J. C., Dasgupta, M., & Marrie, T. J. (1987). Bacterial biofilms in nature and disease. *Annual Review of Microbiology*, *41*, 435–464. https://doi.org/10.1146/annurev.mi.41.100187.002251

Daneshian, B., Höche, D., Knudsen, O. Ø., & Skilbred, A. W. B. (2023). Effect of climatic parameters on marine atmospheric corrosion: correlation analysis of on-site sensors data. *Npj Materials Degradation*, *7*(10). https://doi.org/10.1038/s41529-023-00329-6

Damians, I. P., Bathurst, R. J., Josa, A., Lloret, A., & Albuquerque, P. J. R. (2013). Vertical-facing loads in steel-reinforced soil walls. *Journal of Geotechnical and Geoenvironmental Engineering*, *139*(9), 1419–1432. https://doi.org/10.1061/(ASCE)GT.1943-5606.0000874

Damians, I. P., Bathurst, R. J., Olivella, S., Lloret, A., & Josa, A. (2021). 3D modelling of strip reinforced MSE walls. *Acta Geotechnica*, *16*(3), 711–730. https://doi.org/10.1007/s11440-020-01057-w

Darbin, M., Jailloux, J. M., & Montuelle, J. (1979). Theoretical and practical investigations into the durability of reinforced earth reinforcement. *Bulletin de Liaison des Lab des Ponts et Chaussees*, *99*.

Darbin, M., Jailloux, J. M., & Montuelle, J. (1988). Durability of Reinforced Earth Structures: The Results of a Long-term Study Conducted on Galvanized Steel, *Proc. Institution of Civil Engineers*, Institution of Civil Engineers, Part 1, *84*, 1029-1057.

Davalos, J., Gracia, M., Marco, J. F., & Gancedo, J. R. (1992). Corrosion of weathering steel and iron under wet-dry cycling conditions: Influence of the rise of temperature during the dry period. *Hyperfine Interactions*, *69*, 871–874. https://doi.org/10.1007/BF02401965

DiMaggio, J. A., & MacMillan, A. (2018). A systematic approach to asset management for Mechanically Stabilized Earth walls. In *IFCEE 2018* (pp. 223–231).

Duncan, J. M., & Seed, R. B. (1986). Compaction-induced earth pressures under K_0-conditions. *Journal of Geotechnical Engineering*, *112*(1), 1–22. https://doi.org/10.1061/(ASCE)0733-9410(1986)112:1(1)

Elias, V. (1990). *Durability/corrosion of soil reinforced structures*. Report No. FHWA-RD-89-186, Federal Highway Administration (FHWA).

Elias, V., & Christopher, B.R. (1996). *Mechanically Stabilized Earth walls and reinforced soil slopes, design and construction guidelines*. Report No. FHWA-SA-96-071, Federal Highway Administration.

Elias, V., Christopher, B. R., & Berg, R. R. (2001). *Mechanically Stabilized Earth walls and reinforced soil slopes design and construction guidelines*. Report No. FHWA-NHI-00-043, Federal Highway Administration.

Elias, V., Fishman, K., Christopher, B. R., Berg, R. R., & Berg, R. R. (2009). Corrosion/degradation of soil reinforcements for mechanically stabilized earth walls and reinforced soil slopes (No. FHWA-NHI-09-087). National Highway Institute (US).

Enning, D., Venzlaff, H., Garrelfs, J., Dinh, H. T., Meyer, V., Mayrhofer, K., Hassel, A. W., Stratmann, M., & Widdel, F. (2012). Marine sulfate-reducing bacteria cause serious corrosion of iron under electroconductive biogenic mineral crust. *Environmental Microbiology*, *14*(7), 1772–1787. https://doi.org/10.1111/j.1462-2920.2012.02778.x

Ezuber, H. M., Alshater, A., Hossain, S. Z., & El-Basir, A. (2021). Impact of soil characteristics and moisture content on the corrosion of underground steel pipelines. *Arabian Journal for Science and Engineering*, *46*, 6177–6188. https://doi.org/10.1007/s13369-020-04887-8

FHWA (1987). *Guidelines for the design of Mechanically Stabilized Earth walls (inextensible reinforcements).* FHWA Geotechnical Engineering Notebook Guideline No. 1, Federal Highway Administration.

FHWA (1974). *Standard specifications for construction of roads and bridges on Federal Highway projects*. FP-74, Federal Highway Administration.

FHWA (1979). *Standard specifications for construction of roads and bridges on Federal Highway projects*. FP-79, Federal Highway Administration.

FHWA (1985). *Standard specifications for construction of roads and bridges on Federal Highway projects*. FP-85, Federal Highway Administration.

FHWA (1992). *Standard specifications for construction of roads and bridges on Federal Highway projects*. FP-92, Federal Highway Administration.

Fishman, K. L., & J. L. Withiam. (2011). NCHRP Report 675: LRFD metal loss and service-life strength reduction factors for metal-reinforced systems. Washington, DC: Transportation Research Board.

Fishman, K. L., S. Nazarian, S. Walker, & A. Bronson (2021). *NCHRP Research Report 958: Electrochemical test methods to evaluate the corrosion potential of earthen materials.* Washington, DC: Transportation Research Board

Frondistou-Yannas, F. (1985). *Corrosion susceptibility of internally reinforced soil retaining structures* (No. FHWA-RD-83-105). United States. Department of Transportation. Federal Highway Administration.

Gabr, M. A., Rasdorf, W., Findley, D. J., Butler, C. J., & Bert, S. A. (2018). Comparison of three retaining wall condition assessment rating systems. *Journal of Infrastructure Systems*, *24*(1), 04017037. https://doi.org/10.1061/(ASCE)IS.1943-555X.0000403

Gavin, K., & Igoe, D. (2021). A field investigation into the mechanisms of pile ageing in sand. *Géotechnique*, *71*(2), 120–131. https://doi.org/10.1680/jgeot.18.P.235

Gerber, T. M. (2012). *Assessing the long-term performance of mechanically stabilized earth walls* (Synthesis 437). NCHRP, Transportation Research Board.

Govindasamy, A.V., Marr, A., DiMaggio, J., & Morsy, A.M. (2018), *Risk-based protocol for asset management of Metallically Mechanically Stabilized Earth (MSE) walls.* Report No. FHWA-HIF-18-065, Federal Highway Administration, U.S. Department of Transportation, 109p.

Gupta, S. K., & Gupta, B. K. (1979). The critical soil moisture content in the underground corrosion of mild steel. *Corrosion Science*, *19*(3), 171–178. https://doi.org/10.1016/0010-938X(79)90015-5

Hamilton W. A. (1985). Sulphate-reducing bacteria and anaerobic corrosion. *Annual Review of Microbiology*, *39*, 195–217. https://doi.org/10.1146/annurev.mi.39.100185.001211

Hsuan, Y. G., & Koerner, R. M. (1998). Antioxidant depletion lifetime in high density polyethylene geomembranes. *Journal of Geotechnical and Geoenvironmental Engineering*, *124*, 532–541. https://doi.org/10.1061/(ASCE)1090-0241(1998)124:6(532)

Hubert, C., Nemati, M., Jenneman, G., & Voordouw, G. (2005). Corrosion risk associated with microbial souring control using nitrate or nitrite. *Applied Microbiology and Biotechnology*, *68*, 272–282. https://doi.org/10.1007/s00253-005-1897-2

Itasca (2019). *FLAC – Fast Lagrangian Analysis of Continua, Version 8.1*. Itasca Consulting Group, Inc., Minneapolis, MN.

Kennedy, V. C. (1965). *Mineralogy and cation-exchange capacity of sediments from selected streams*. US Government Printing Office.

Kibria, G., Hossain, M. S., & Khan, M. S. (2014). Influence of soil reinforcement on horizontal displacement of MSE wall. *International Journal of Geomechanics*, *14*(1), 130–141. https://doi.org/10.1061/(ASCE)GM.1943-5622.0000297

Kolay, P. K., Tajhya, D., & Mondal, K. (2020). Corrosion of steel in MSE walls due to deicers and backfill aggregates. *Geotechnical and Geological Engineering*, *38*(3), 2493–2507. https://doi.org/10.1007/s10706-019-01164-w

Kwok, C. Y., & Bolton, M. D. (2013). DEM simulations of soil creep due to particle crushing. *Géotechnique, 63*(16), 1365–1376. https://doi.org/10.1680/geot.11.P.089

Lajvardi, V., & Dias, D. (2021). Impact of rainfall infiltration on the stability of Mechanically Stabilized Earth walls: A numerical study. *Journal of Geotechnical and Geoenvironmental Engineering*, *147*(4), 04021010.

Lefebvre, G., & Duncan, J. M. (1971). *Three-dimensional finite element analyses of dams*, Contract Rep. s-71-6, U.S. Army Engr. Wtwys. Experiment St., Vicksburg, Miss.

Lim, S. Y., & McCartney, J. S. (2013). Evaluation of effect of backfill particle size on installation damage reduction factors for geogrids. *Geosynthetics International*, *20*(2), 62–72. https://doi.org/10.1680/gein.13.00002

Liu, S., Wang, J., & Kwok, C. Y. (2019). DEM simulation of creep in one-dimensional compression of crushable sand. *Journal of Geotechnical and Geoenvironmental Engineering*, *145*(10), 04019060. https://doi.org/10.1061/(ASCE)GT.1943-5606.0002098

Liu, C., Tai, P., Li, Z., & Hu, W. (2022). Mechanism of packing rigidity gain in sand aging: From the perspective of structural order evolution. *KSCE Journal of Civil Engineering*, *26*(6), 2641–2652. https://doi.org/10.1007/s12205-022-1460-z

Liu, L., Li, W., Deng, Z., Xu, S., Xu, Y., Zeng, L., Li, D., Yang, Y., & Zhong, Z. (2023). Effect of moisture on corrosion behavior of Q235 steel in bentonite clay. *International Journal of Electrochemical Science*, *18*(6), 100164. https://doi.org/10.1016/j.ijoes.2023.100164

Merritt, A. J., Chambers, J. E., Wilkinson, P. B., West, L. J., Murphy, W., Gunn, D., & Uhlemann, S. (2016). Measurement and modelling of moisture—electrical resistivity relationship of fine-grained unsaturated soils and electrical anisotropy. *Journal of Applied Geophysics*, *124*, 155–165. https://doi.org/10.1016/j.jappgeo.2015.11.005

Mitchell, J. K., & Villet, W. C. (1987). *Reinforcement of earth slopes and embankments*. NCHRP Report 290. Transportation Research Board of the National Academies, Washington, D.C.

Miyata, Y., & Bathurst, R. J. (2015). Reliability analysis of geogrid installation damage test data in Japan. *Soils and Foundations*, *55*(2), 393–403. https://doi.org/10.1016/j.sandf.2015.02.013

Morsy, A.M., Helm, P.R., El-Hamalawi, A., Smith, A., Hughes, P.N., Stirling, R.A., & Glendinning, S. (2023). Development of a multiphase numerical modeling approach for hydromechanical behavior of clay embankments subject to weather-driven deterioration. *Journal of Geotechnical and Geoenvironmental Engineering*, *149*(8), 04023062. https://doi.org/10.1061/JGGEFK.GTENG-11213

Morsy, A.M., & Helm, P.R. (2024). Failure prediction of clay embankments subject to weather-driven deterioration. *Journal of Geotechnical and Geoenvironmental Engineering*, *150*(12). https://doi.org/10.1061/JGGEFK.GTENG-12842

Mualem, Y. (1976). A new model for predicting the hydraulic conductivity of unsaturated porous media. *Water Resources Research*, *12*(3), 513–522. https://doi.org/10.1029/WR012i003p00513

Mughabghab, S. F., & Sullivan, T. M. (1989). Evaluation of the pitting corrosion of carbon steels and other ferrous metals in soil systems. *Waste Management*, *9*(4), 239–251. https://doi.org/10.1016/0956-053X(89)90408-X

NASEM (2023). *Development of guidance for the use of non-destructive testing in transportation asset management*. Project 26686, National Academies of Sciences, Engineering, and Medicine, Washington, D.C., 129p.

Nicks, J. E., Adams, M. T., Stabile, T., & Ocel, J. (2017). Case study: Condition assessment of a 36-year-old mechanically stabilized earth wall in Virginia. *Journal of Geotechnical and Geoenvironmental Engineering*, *143*(5), 05016003. https://doi.org/10.1061/(ASCE)GT.1943-5606.0001648

Noor, E. A., & Al-Moubaraki, A. H. (2014). Influence of soil moisture content on the corrosion behavior of X60 steel in different soils. *Arabian Journal for Science and Engineering*, *39*, 5421–5435. https://doi.org/10.1007/s13369-014-1135-2

NYSDOT (2018). *Retaining wall inventory and inspection program*. State of New York Department of Transportation.

Palmerton, J.B., & Lefebvre, G. (1972). *Three-dimensional finite element analyses of dams.* Rep. No. S 72-1, U.S. Army Engineers Waterways Experiment Station, Corps of Engineers, Vicksburg, MS.

Parker, J. C., Lenhard, R. J., & Kuppusamy, T. (1987). A parametric model for constitutive properties governing multiphase flow in porous media. *Water Resources Research*, *23*(4), 618–624. https://doi.org/10.1029/WR023i004p00618

Qi, Y., Luo, H., Zheng, S., Chen, C., Lv, Z., & Xiong, M. (2014). Effect of temperature on the corrosion behavior of carbon steel in hydrogen sulphide environments. *International Journal of Electrochemical Science*, *9*(4), 2101–2112. https://doi.org/10.1016/S1452-3981(23)07914-2

Rehm, G. (1980), *The service life of reinforced earth structures from a corrosion technology standpoint*, Expert Report, The Reinforced Earth Company, Vienna, Virginia.

Roberge, P. (2000). *Handbook of corrosion engineering.* New York: McGraw-Hill Education.

Romanoff, M. (1956). *Underground Corrosion.* National Bureau of Standards Circular 579, U.S. Department of Commerce, Washington, D.C., 166p.

Rossum, J. R. (1969). Prediction of pitting rates in ferrous metals from soil parameters. *Journal-American Water Works Association*, *61*(6), 305–310. https://doi.org/10.1002/j.1551-8833.1969.tb03761.x

Rowe, R. K., & Sangam, H. P. (2002). Durability of HDPE geomembranes. *Geotextiles and Geomembranes*, *20*(2), 77–95. https://doi.org/10.1016/S0266-1144(02)00005-5

Rowe, R. K. (2020). Protecting the environment with geosynthetics: 53rd Karl Terzaghi Lecture. *Journal of Geotechnical and Geoenvironmental Engineering*, *146*(9), 04020081. https://doi.org/10.1061/(ASCE)GT.1943-5606.0002239

Sabatini, P. J., Pass, D. G., & Bachus, R. C. (1999). *Ground anchors and anchored systems* (No. FHWA-IF-99-015). United States. Federal Highway Administration. Office of Bridge Technology.

Sanford Bernhardt, K. L., Loehr, J. E., & Huaco, D. (2003). Asset management framework for geotechnical infrastructure. *Journal of Infrastructure Systems*, *9*(3), 107–116. https://doi.org/10.1061/(ASCE)1076-0342(2003)9:3(107)

Shreir, L. L., R. A. Jarman, and G. T. Burstein (1994). *Corrosion*, vol. 1, 3rd ed. Oxford, UK: Butterworth Heinemann Ltd.

Sibille, L., Marot, D., & Sail, Y. (2015). A description of internal erosion by suffusion and induced settlements on cohesionless granular matter. *Acta Geotechnica*, *10*, 735–748. https://doi.org/10.1007/s11440-015-0388-6

TAMP (2022). *California transportation asset management plan*. California Department of Transportation (Caltrans).

Tarawneh, B., Al Bodour, W., & Masada, T. (2018). Inspection and risk assessment of mechanically stabilized earth walls supporting bridge abutments. *Journal of Performance of Constructed Facilities*, *32*(1), 04017131. https://doi.org/10.1061/(ASCE)CF.1943-5509.0001132

Taylor, T.P., Collin, J.G., Boyle, S., Fishman, K., & Han, J. (2023). *Design and construction of Mechanically Stabilized Earth (MSE) walls*. FHWA GEC 011, Federal Highway Administration, U.S. Department of Transportation, Washington, D.C., 429p.

Telford, W. M., Geldart, L. P., & Sheriff, R. E. (1990). Applied geophysics. Cambridge University Press.

Terre Armee Internationale (1982). *Durabilite de l'Acier galvanise enterre*. Rapport R25, December.

van Genuchten, M. T. (1980). A closed-form equation for predicting the hydraulic conductivity of unsaturated soils. *Soil Science Society of America Journal*, *44*(5), 892–898. https://doi.org/10.2136/sssaj1980.03615995004400050002x

Vessely, M., Robert, W., Richrath, S., Schaefer, V. R., Smadi, O., Loehr, E., & Boeckmann, A. (2019a). *Geotechnical asset management for transportation agencies, volume 1: Research overview*. *NCHRP Research Report*, (Project 24-46).

Vessely, M., Robert, W., Richrath, S., Schaefer, V. R., Smadi, O., Loehr, E., & Boeckmann, A. (2019b). *Geotechnical asset management for transportation agencies, volume 2: Implementation manual* (No. Project 24-46).

Walkinshaw, J.L. (1975). *Reinforced earth construction*. Report No. FHWA-DP-18. Region I5 Demonstration Project No. 18, Federal Highway Administration.

Wasim, M., Shoaib, S., Mubarak, N. M., Inamuddin, & Asiri, A. M. (2018). Factors influencing corrosion of metal pipes in soils. *Environmental Chemistry Letters*, *16*, 861–879. https://doi.org/10.1007/s10311-018-0731-x

Waxman, M. H., & Smits, L. J. M. (1968). Electrical conductivities in oil-bearing shaly sands. *Society of Petroleum Engineers Journal*, *8*(02), 107–122. https://doi.org/10.2118/1863-A

Worthington, P. F. (1993). The uses and abuses of the Archie equations, 1: The formation factor-porosity relationship. *Journal of Applied Geophysics*, *30*(3), 215–228. https://doi.org/10.1016/0926-9851(93)90028-W

Xiang, Y., Wang, Z., Li, Z., & Ni, W. D. (2013). Effect of temperature on corrosion behaviour of X70 steel in high pressure $CO_2/SO_2/O_2/H_2O$ environments. *Corrosion Engineering, Science and Technology*, *48*(2), 121–129. https://doi.org/10.1179/1743278212Y.0000000050

Yu, Y., Bathurst, R. J., & Miyata, Y. (2015). Simplified method for estimating loads in reinforced soil walls subject to external water pressure. *Journal of Geotechnical and Geoenvironmental Engineering*, *141*(6), 04015023.

Zevgolis, I. E., & Bourdeau, P. L. (2007). Mechanically Stabilized Earth wall abutments for bridge support. *Journal of Performance of Constructed Facilities*, *21*(6), 481–489.

About the Authors

Amr M. Morsy, PhD, PE

Dr. Amr Morsy is a professional civil engineer with experience in both academia and industry. His research focuses on geotechnical engineering, transportation geotechnics, environmental geotechnics, and climate adaptation. He obtained his B.Eng and M.Sc. degrees in civil engineering from Cairo University in 2011 and 2013 respectively and obtained his PhD degree in civil engineering from The University of Texas at Austin in 2017. He worked as a postdoctoral fellow at The University of Texas at Austin in 2018 and as a practicing geotechnical engineer from 2018 to 2020. He later worked as a research associate at Loughborough University on the ACHILLES program grant from 2020 to 2022. He has been working as an assistant professor at California State University, Long Beach since 2022.

As part of his academic experience, Dr. Morsy conducts research on geotechnical infrastructure deterioration and asset management, climate change impacts on geotechnical infrastructure, and geotechnical solutions for sustainable built environments. He has excelled in physical and numerical modeling of geotechnical and geoenvironmental engineering systems, and in infrastructure instrumentation and laboratory experimentation. He participated in research projects sponsored by the Transportation Research Board of the National Academies of Sciences, Engineering, and Medicine, the Engineering and Physical Sciences Research Council of the UK Research and Innovation, the US Federal Highway Administration, the Geosynthetic Institute, the Departments of Transportation of Texas and Indiana, and geosynthetic manufacturers.

As part of his professional consulting experience, Dr. Morsy conducts rigorous analyses, designs, and forensic evaluations for a range of slopes, retaining walls, reinforced soil structures, deep excavations, bridge foundations, waste containment facilities, tailings dams, and embankment dams. He assisted expert witnesses in cases involving collapse and poor performance of earth retaining structures. He provided solutions to geotechnical problems in a number of environmental remediation projects involving cleanup of superfund sites. He conducted multi-phase flow analyses for several infrastructure features including earthworks, embankment dams, and cover systems. Some of the consulting projects he participated in served the US Environmental Protection Agency, New York State Department of Environmental Conservation, New York State and Indiana Departments of Transportation, Tennessee Valley Authority, New Jersey Transit, and several multinational private and public corporates.

Islam A. Ebo

Islam Ahmed is a marine and geotechnical engineer with experience in both industry and academic research. He obtained his bachelor's degree in civil engineering from Alexandria University in 2018 and is currently pursuing a master's degree in geotechnical engineering at California State University, Long Beach.

Islam has worked on a variety of large-scale civil and geotechnical engineering projects with a focus on infrastructure development, particularly in marine and coastal environments. His work involves using advanced engineering tools to ensure the structural stability and environmental sustainability of these projects.

In his research role, Islam is focused on studying soil-structure interactions, coastal protection strategies, and the effects of environmental factors on marine infrastructure. He has developed strong skills in geotechnical analysis, project management, and field assessments, working closely with multidisciplinary teams to address engineering challenge.

MTI FOUNDER

Hon. Norman Y. Mineta

MTI BOARD OF TRUSTEES

Directors

MTI MINETA TRANSPORTATION INSTITUTE